Radio wave propagation for communication and probing the ionosphere

Norbert Jakowski

Institute of Communications
and Navigation

German Aerospace Center

DLR

Outline

- Introduction
- Radio wave propagation and ionosphere
  - The ionosphere
  - Fundamentals of radio wave propagation
- Probing the ionosphere and space weather relationships
  - Ground based
  - Radio occultation
  - Topside ionosphere/plasmasphere monitoring
  - Observations
- Ionospheric impact on radio systems and mitigation techniques
  - Telecommunication
  - Remote sensing
  - Space based navigation
- Summary and conclusions

DLR

Radio systems are vulnerable against space weather

Radio waves play a significant role in various modern technological systems:

- Terrestrial and space based telecommunication
- Ground and space based navigation systems (e.g. GNSS)
- Remote sensing radars

Radio wave propagation is closely related to ionospheric conditions in most applications.

Ionosphere is impacted by space weather and associated coupling with magnetosphere and thermosphere.

Positioning, Navigation &Timing (PNT) play a significant role in the modern society

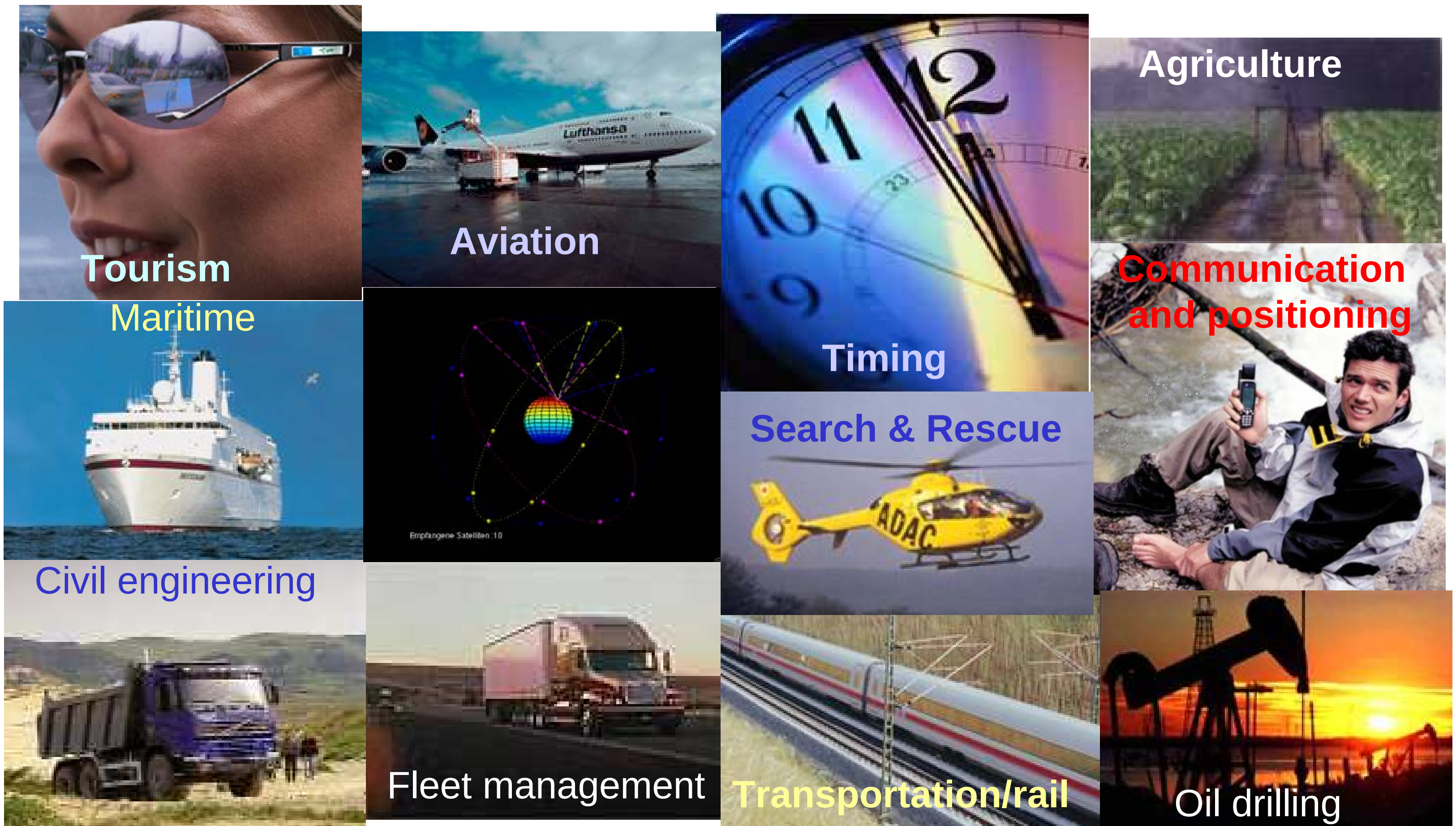

Outline

- Introduction
- Radio wave propagation and ionosphere
  - The ionosphere
  - Fundamentals of radio wave propagation
- Probing the ionosphere and space weather relationships
  - Ground based
  - Radio occultation
  - Topside ionosphere/plasmasphere monitoring
  - Observations
- Ionospheric impact on radio systems and mitigation techniques
  - Telecommunication
  - Remote sensing
  - Space based navigation
- Summary and conclusions

Radio wave propagation & Ionosphere (II)

- G. Marconi (1901), first transatlantic radio transmission, assumption of an electrically conductive layer in the atmosphere (Kennelly-Heaviside Layer)
- R.A. Watson Watt (1926), suggestion to call the electrically active part of the atmosphere ‚**Ionosphere**'
- E.V. Appleton (1927- 32), **Theory of radio wave propagation in plasma**

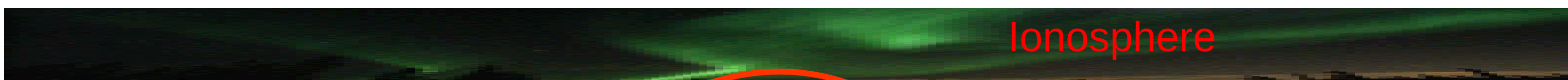

3500 km

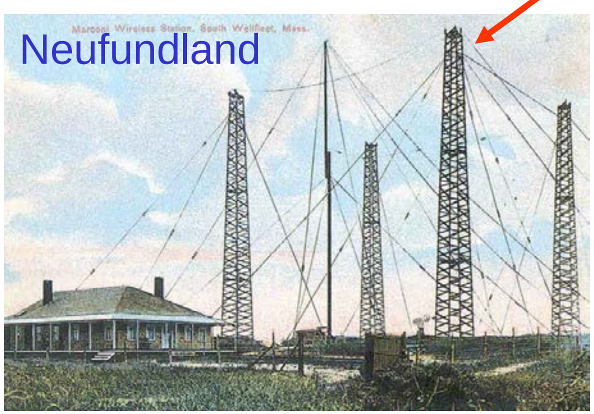

Ionospheric research starts practically with these transmission experiments.

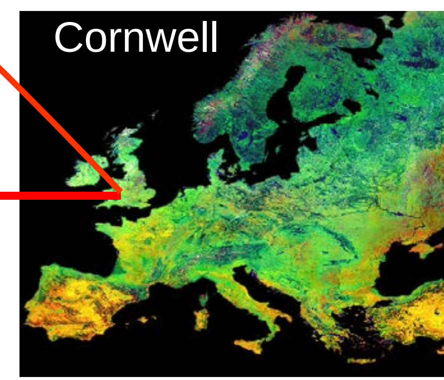

Radio wave propagation & Ionosphere (I)

EDWARD V. APPLETON
The ionosphere
Nobel Lecture, December 12, 1947

„Now the most striking feature of the atmospheric air at high levels is that it is ionized, and for that reason the spherical shell surrounding the earth at the levels with which we are concerned is called the ionosphere.“

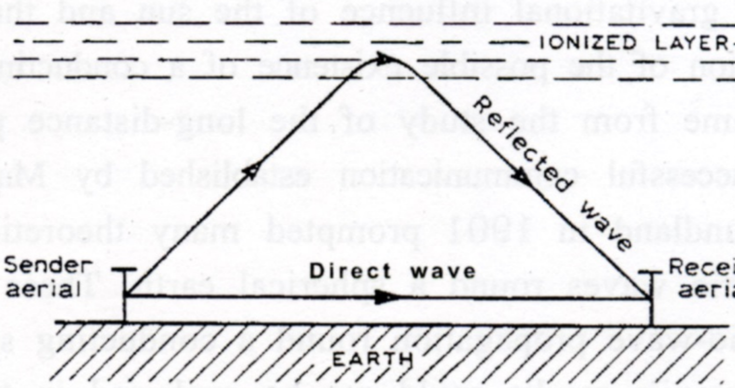

Fig. I.

The Ionosphere - integral part of the Geo-sphere

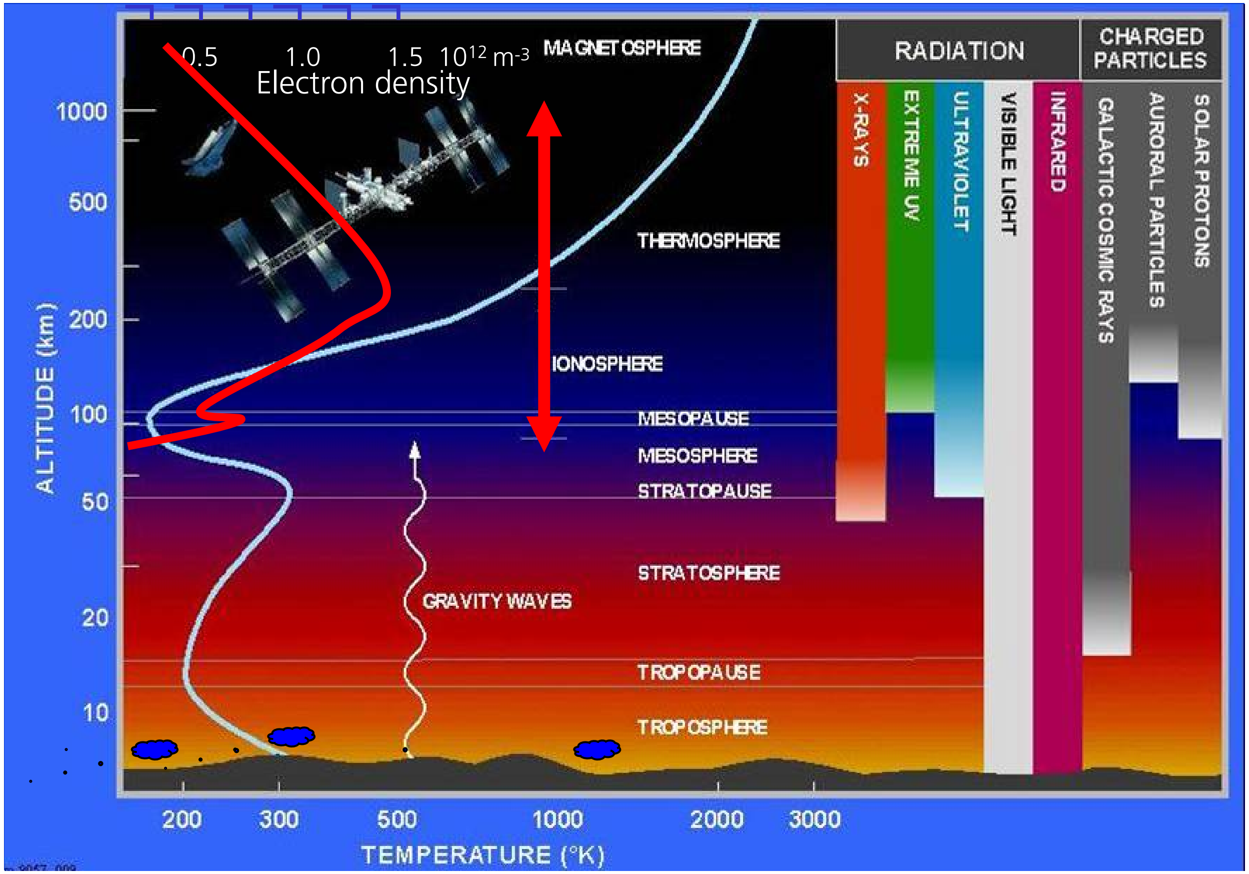

The Ionosphere ist integral part of the Earth's environment (strong coupling with other Geo-spheres).

The ionospheric plasma is mainly formed by solar radiation at wavelengths < 130 nm.

Solar storms and associated Coronal Mass Ejections (CMEs) may heavily disturb the ionospheric behaviour.

Ionosphere and radio waves

$$TEC = \int n_e(h)\ dh$$

Continuity equation for the electron gas

$$\frac{\partial n_e}{\partial t} = Q - L - div\ (n_e \cdot v)$$

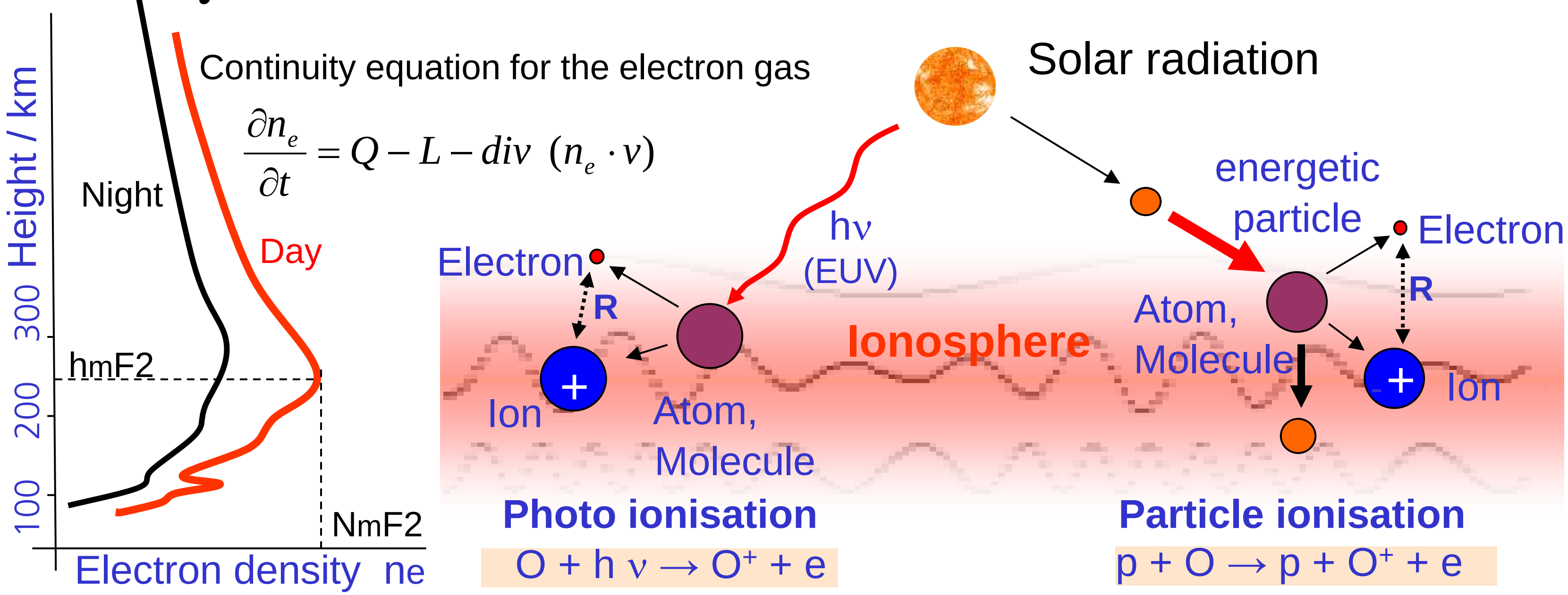

- Ionospheric ionisation is generated by solar radiation and energetic particles and by galactic cosmic rays (Space weather dependence).
- Strong coupling with thermosphere and magnetosphere.
- Charged particles of ionosphere impact propagation of electromagnetic radio waves.

Refractive index of ionospheric plasma (f >> f_p) (Appleton-Lassen-Hartree)

$$n = 1 - \frac{f_p^2}{2f^2} \pm \frac{f_p^2 f_g \cos\Theta}{2f^3} - \frac{f_p^4}{8f^4}$$

first-order second-order third-order term

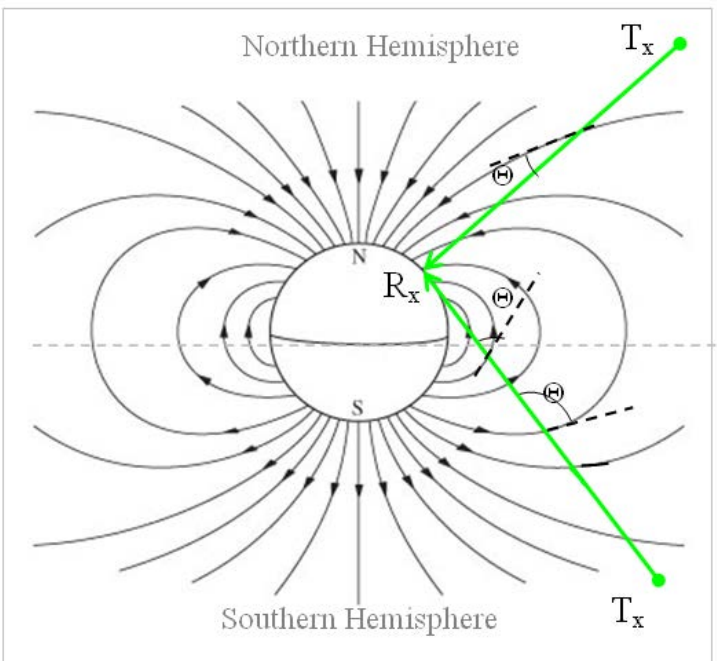

Plasma frequency:

$$f_p = \sqrt{e^2 n_e /(4\pi^2 m_e \varepsilon_0)}$$

Gyro frequency:

$$f_g = eB/2\pi \cdot m_e$$

Θ: angle between wave direction and B field vector; n_e: electron density
m_e: electron mass; B: magnetic induction
ε_0: free space permitivity
f : signal frequency

[REF 01, 02]

Radio frequency ranges & propagation

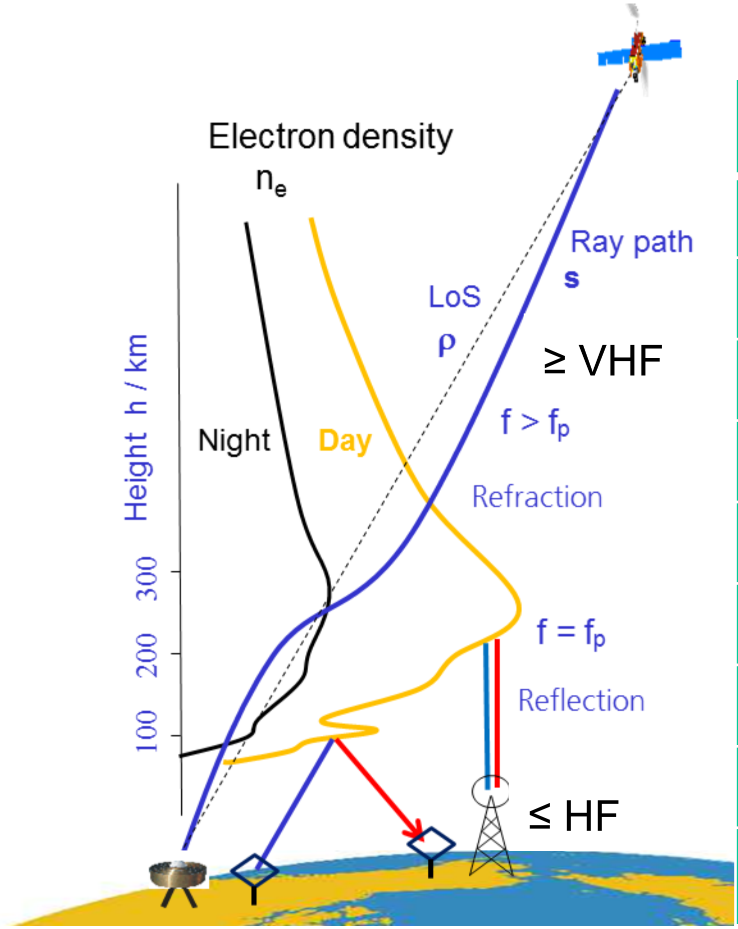

Symbol of frequency band	Frequency range	Wavelength range
ELF Extreme Low Frequency	< 300 Hz	> 1000 km
ULF Ultra Low Frequency	300 Hz - 3 kHz	1000 - 100 km
VLF Very Low Frequency	3 kHz - 30 kHz	100 - 10 km
LF Low Frequency	30 kHz - 300 kHz	10 - 1 km
MF Medium Frequency	300 kHz - 3 MHz	1000 - 100 m
HF High Frequency	3 MHz - 30 MHz	100 - 10 m
VHF Very High Frequency	30 MHz - 300 MHz	10 - 1 m
UHF Ultra High Frequency	300 MHz - 3 GHz	1000 - 100 mm
SHF Super High Frequency	3 GHz - 30 GHz	100 - 10 mm

Transionospheric propagation of radio waves

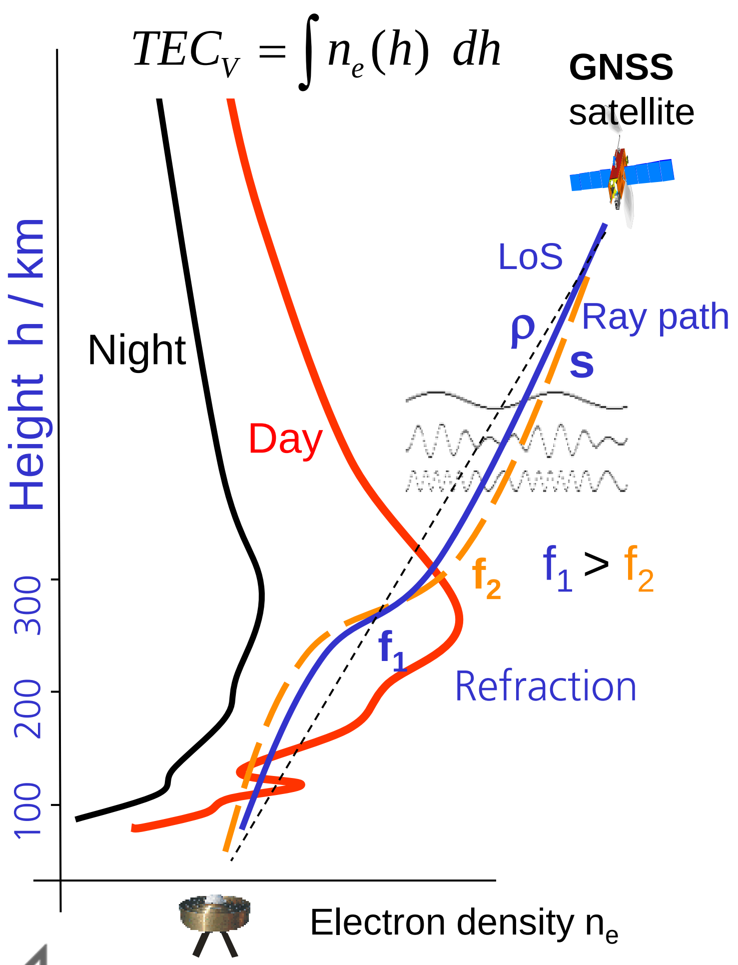

Refraction of radio waves transmitted by satellites of Global Navigation Satellite Systems (GNSS):

The phase length L along the ray path s is defined by the integral

$$L = \int n\ ds \ = Min$$

where n is the refractive index and the integral becomes a minimum according to Fermat‘s principle.

For GNSS, the phase length can be written:

$$L = \int (n - 1)\ ds + \rho + \Delta s_B$$

where ρ is the line of sight and Δs_B means the excess path due to bending.

Observation equations of GNSS measurements

Neglecting higher order terms in the refractive index and bending, the observation equations of GNSS measurements for code phases P_1/P_2 and L_1/L_2 carrier phases can be written:

$$P = \boxed{\rho} + c(\Delta t_{rec} - \Delta t^{sat}) + d_T + \boxed{d_I} + d_{MP} + \varepsilon_P$$

$$\Phi = \boxed{\rho} + c(\Delta t_{rec} - \Delta t^{sat}) + d_T - \boxed{d_I} + d_{MP} + N_a \lambda + \varepsilon_\Phi$$

ρ	**true range between GPS satellite and receiver along ray path s**
c	velocity of light
Δt^{sat}	offset of satellite clock from GNSS Time
Δt_{rec}	offset of receiver clock from GNSS Time
d_I	**ionospheric phase delay along s**
d_T	atmospheric phase delay along s
d_{MP}	error due to multipath
λ	wave length of radio wave
N_a	phase ambiguity number (integer)
ε	Phase noise

$$d_I = \frac{K}{f^2} \cdot TEC_S$$

Ionospheric range error

$$K = 40.3 \ m^3 s^{-2}$$

Ionosphere related range errors deduced from dual-frequency GNSS measurements

$$TEC = \int n_e(h)\ dh$$

$$M(\varepsilon) = \frac{TEC_S}{TEC}$$

$$\Delta P = P_2 - P_1 = K\,\frac{f_1^{\,2} - f_2^{\,2}}{f_1^{\,2} f_2^{\,2}}\,TEC_S + \varepsilon_{off}$$

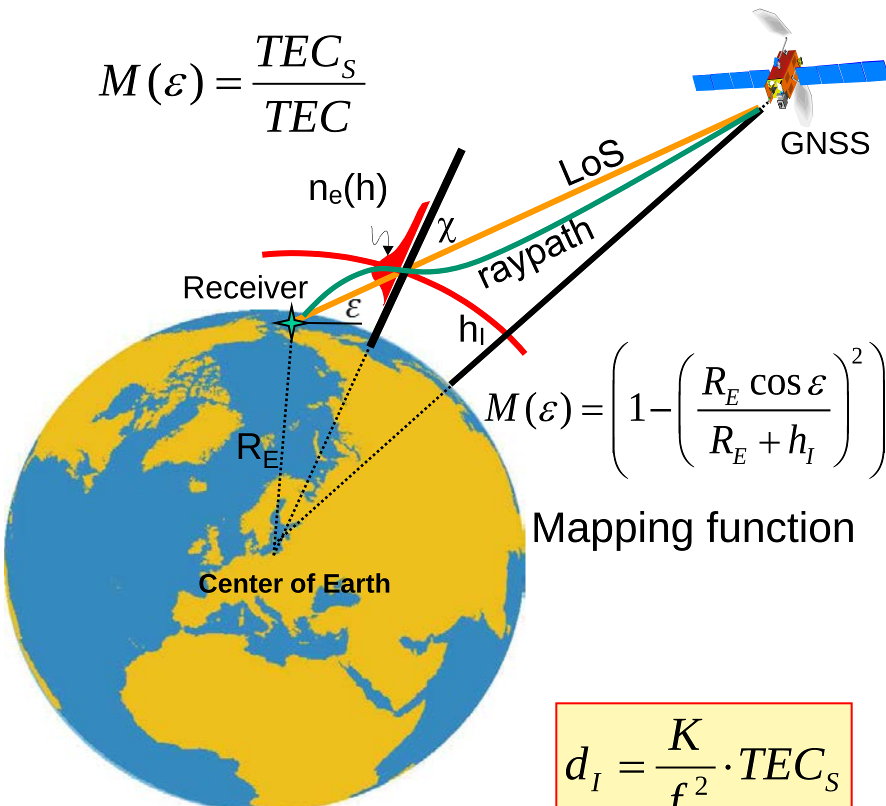

$$M(\varepsilon) = \left(1 - \left(\frac{R_E \cos\varepsilon}{R_E + h_I}\right)^2\right)^{-1/2}$$

Mapping function

$$d_I = \frac{K}{f^2} \cdot TEC_S$$

Due to the dispersive ionosphere TEC can be derived from dual-frequency GNSS measurements (differential phases).

The ionospheric range error d_I is the biggest error source in single frequency GNSS applications (up to 100 m along ray path).

Single-frequency measurements need range error correction information from:

- TEC monitoring data (map) or
- TEC model computations

Outline

- Introduction
- Radio wave propagation and ionosphere
    - The ionosphere
    - Fundamentals of radio wave propagation
- Probing the ionosphere and space weather relationships
    - Ground based
    - Radio occultation
    - Topside ionosphere/plasmasphere monitoring
    - Observations
- Ionospheric impact on radio systems and mitigation techniques
    - Telecommunication
    - Remote sensing
    - Space based navigation
- Summary and conclusions

Computation of the Total Electron Content (TEC)

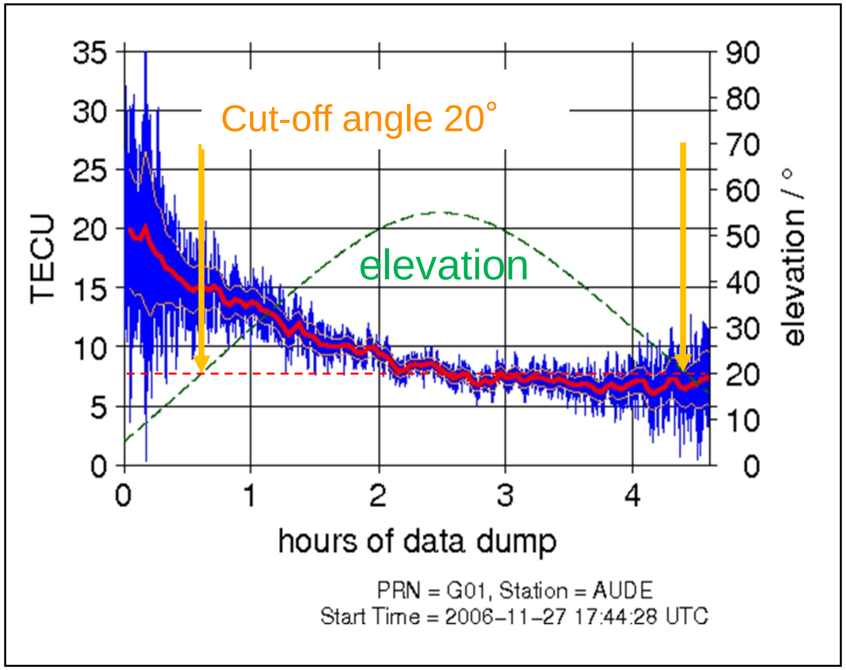

$$P_2 - P_1 = \frac{K(f_1^2 - f_2^2)}{f_1^2 \cdot f_2^2} TEC_S + \varepsilon_{Poff}$$

$$\Phi_1 - \Phi_2 = \frac{K(f_1^2 - f_2^2)}{f_1^2 \cdot f_2^2} TEC_S + \varepsilon_{\Phi off}$$

$$K = 40.3 \; m^3 s^{-2}$$

GPS f_1=1575.42 MHz
f_2=1227.60 MHz

$$TEC_S = \frac{f_1^2 \cdot f_2^2}{K(f_1^2 - f_2^2)} (\Phi_1 - \Phi_2) + B + \varepsilon_N$$

After levelling relative carrier phase differences into absolute uncalibrated code phase differences, subsequent TEC computation uses only carrier phases.

[REF 03, 04]

Generation of TEC maps

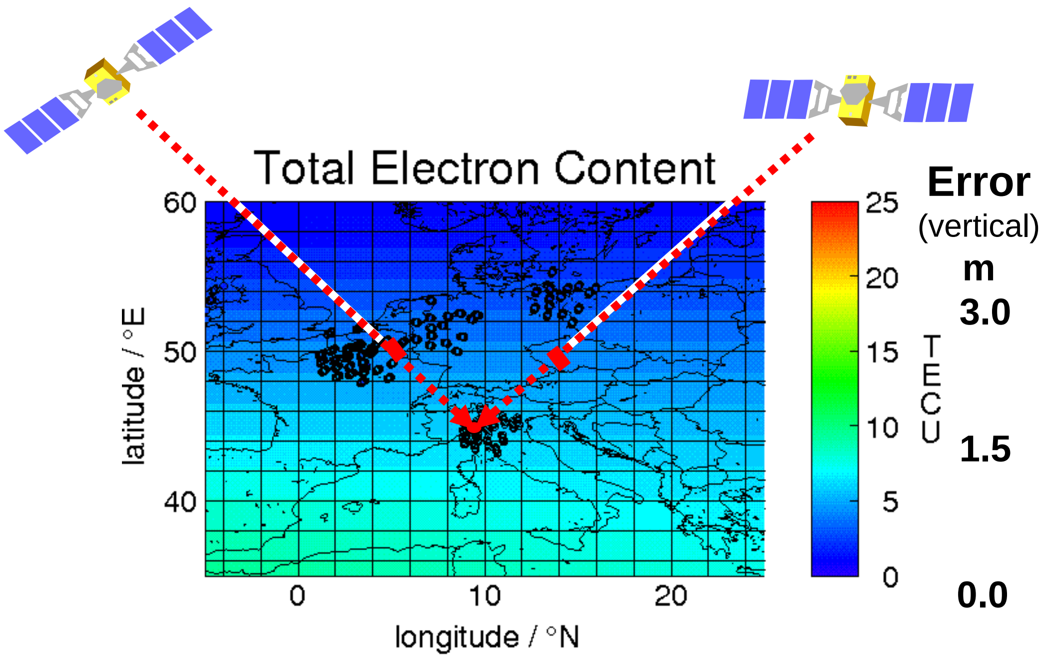

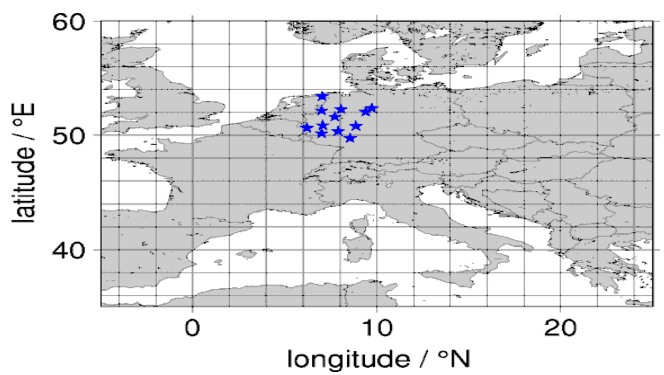

- Assimilation of calibrated TEC data into a background model of TEC to generate TEC maps
- Procedure allows extrapolating TEC into areas without measurements.
- Accuracy increases with number of used stations (here:16)

[REF 04]

Space Based Sounding of the Ionosphere

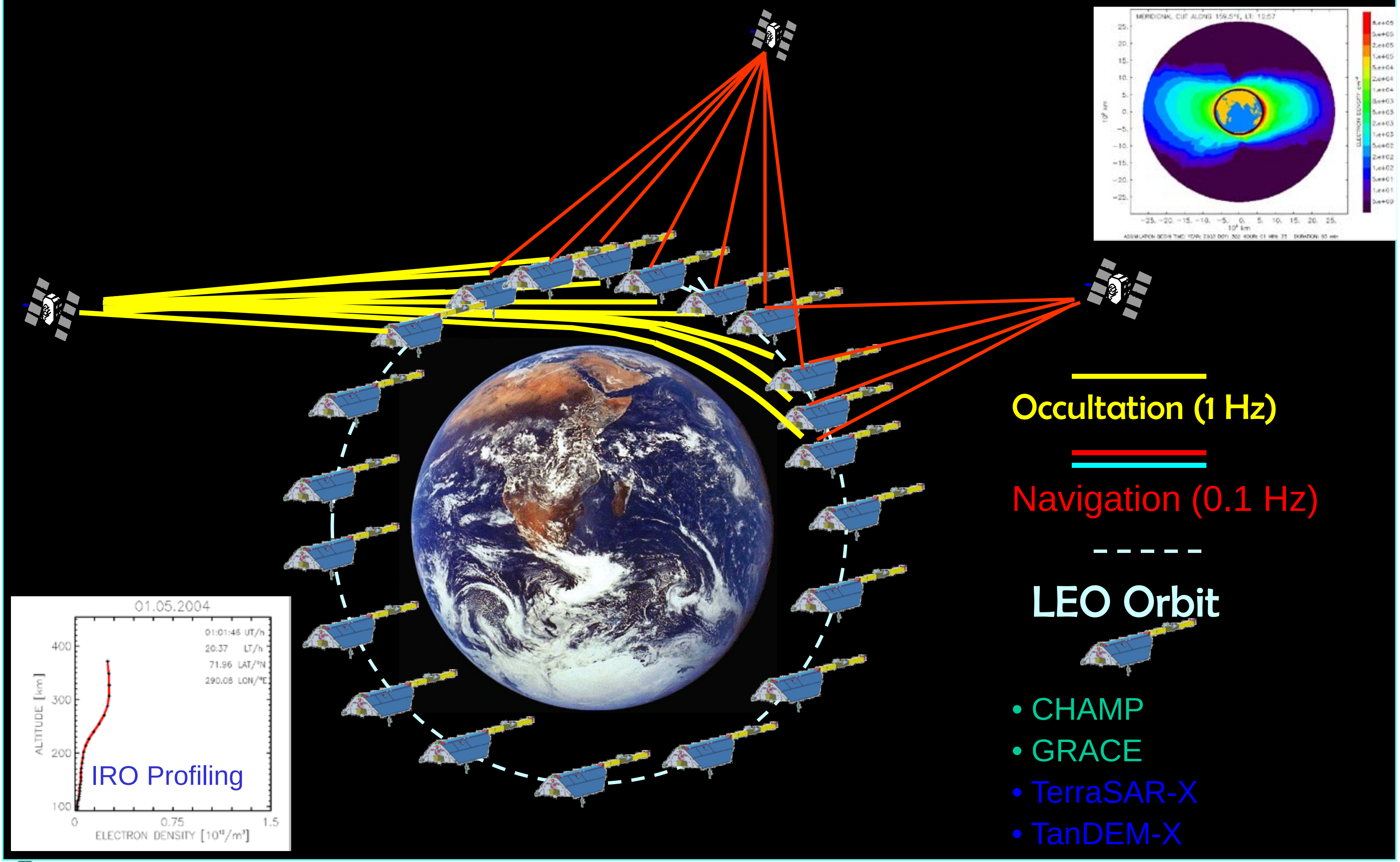

History of radio occultation

1960's Exploration of planetary atmospheres using tracking and telemetry signals of deep space missions

Martian atmosphere — Mariner IV

Venus atmosphere — Mariner V, Venera 4

1980's Sounding of planetary atmospheres of Jupiter, Saturn, Uranus

Proposal for using the GPS system for sounding the Earth's atmosphere

1990's Demonstration of the capabilities for Earth's atmosphere sounding

Use of Salyut stations for exploring the Earth's atmosphere by radio occultation (RO) techniques

GPS/MET experiment onboard Microlab 1 led by UCAR/USA as a proof-of-concept mission launched in April 1994

2000's Several satellite missions enabling GPS radio occultation

Launch of CHAMP led by GFZ Potsdam

Launch of SAC-C led by NASA/JPL

COSMIC, GRACE, TerraSAR-X, Tandem-X

DLR

RO satellite missions CHAMP - GRACE - COSMIC

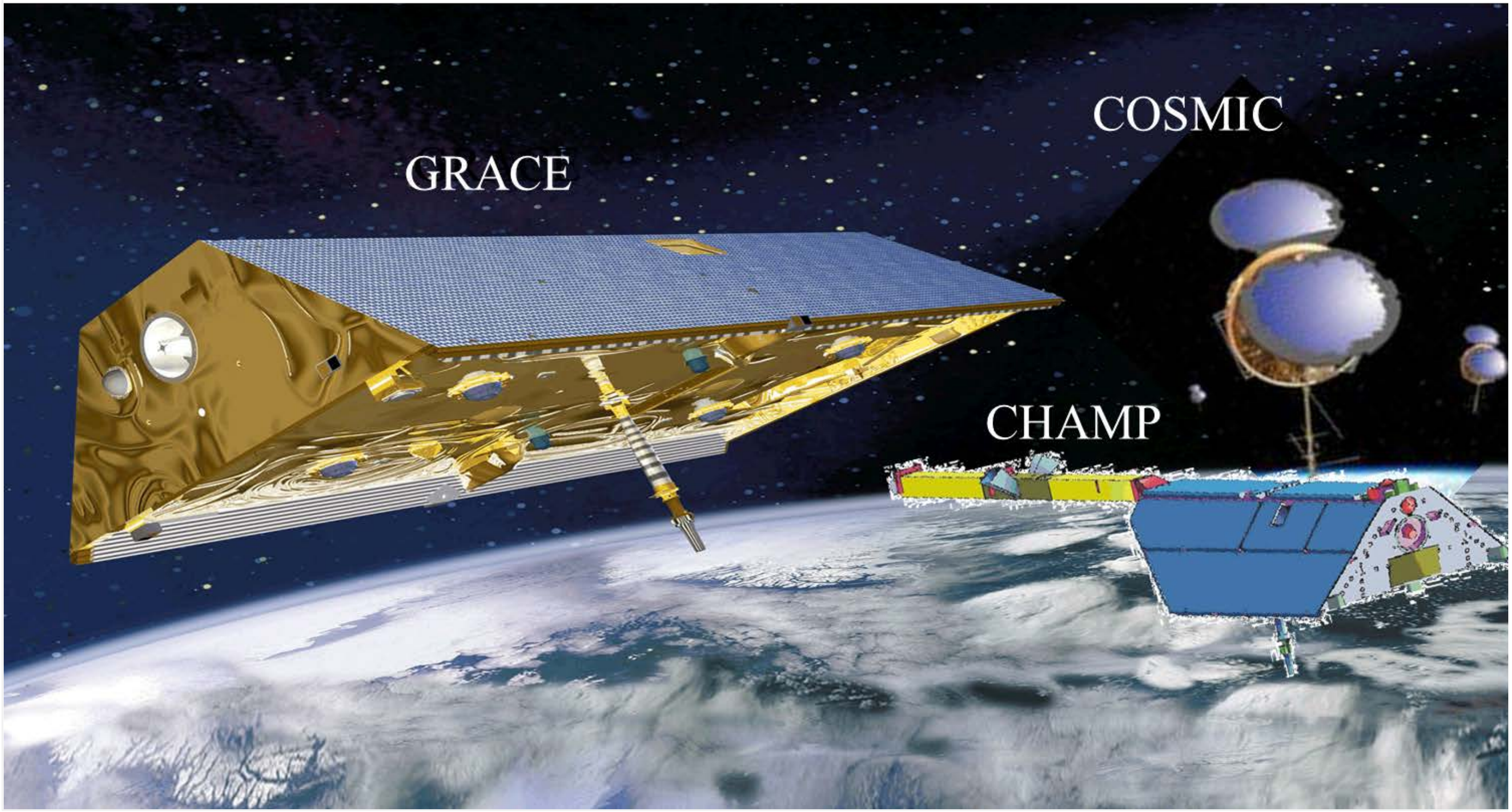

GNSS radio occultation
Retrieval of electron density profiles (I)

Topside ionosphere/plasmasphere $n_e \sim \exp(-h/H_S)$

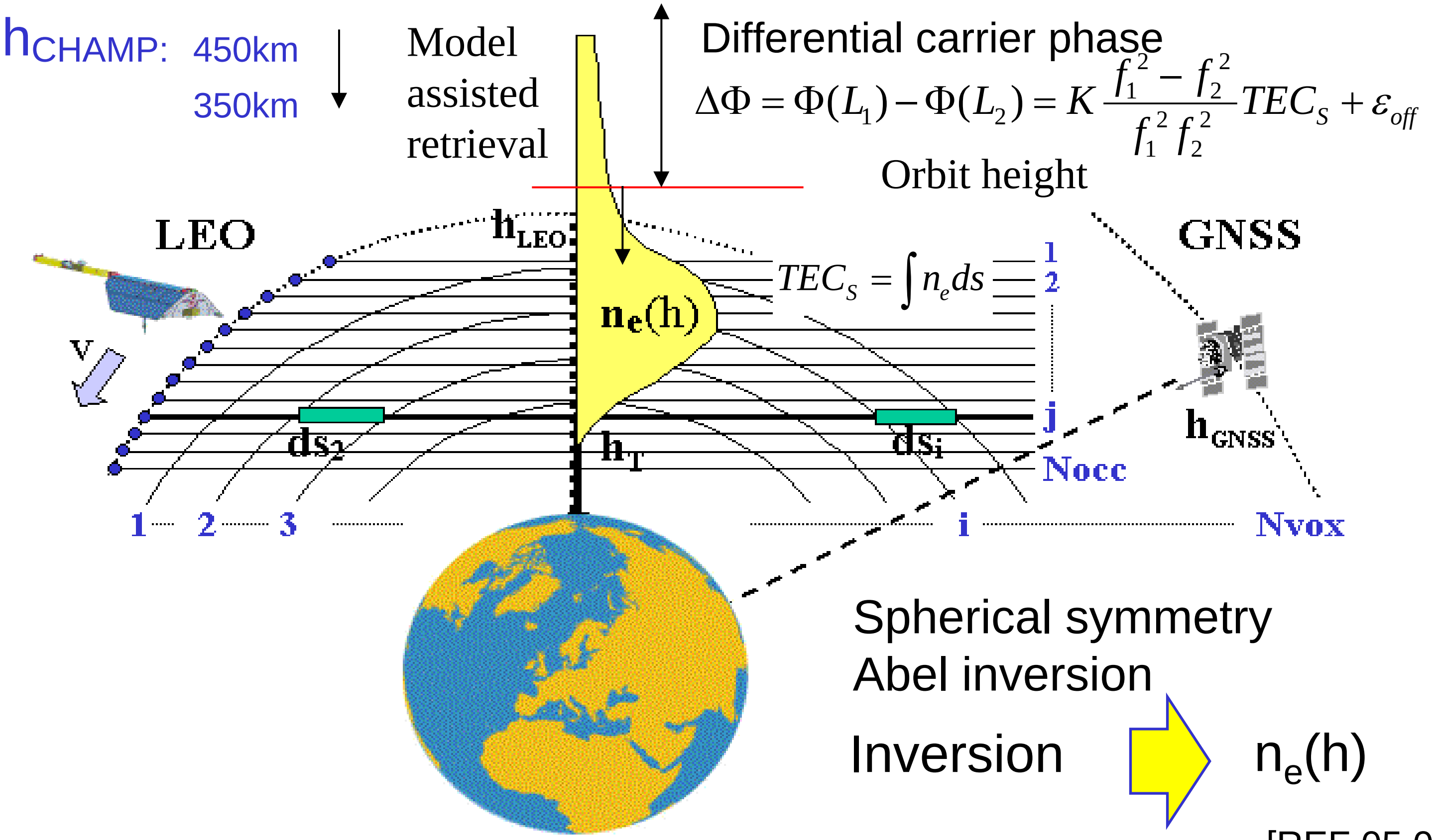

Spherical symmetry
Abel inversion

Inversion ⇒ $n_e(h)$

[REF 05,06,07,08]

Review of vertical electron density profiles obtained from CHAMP

High solar activity | Low solar activity

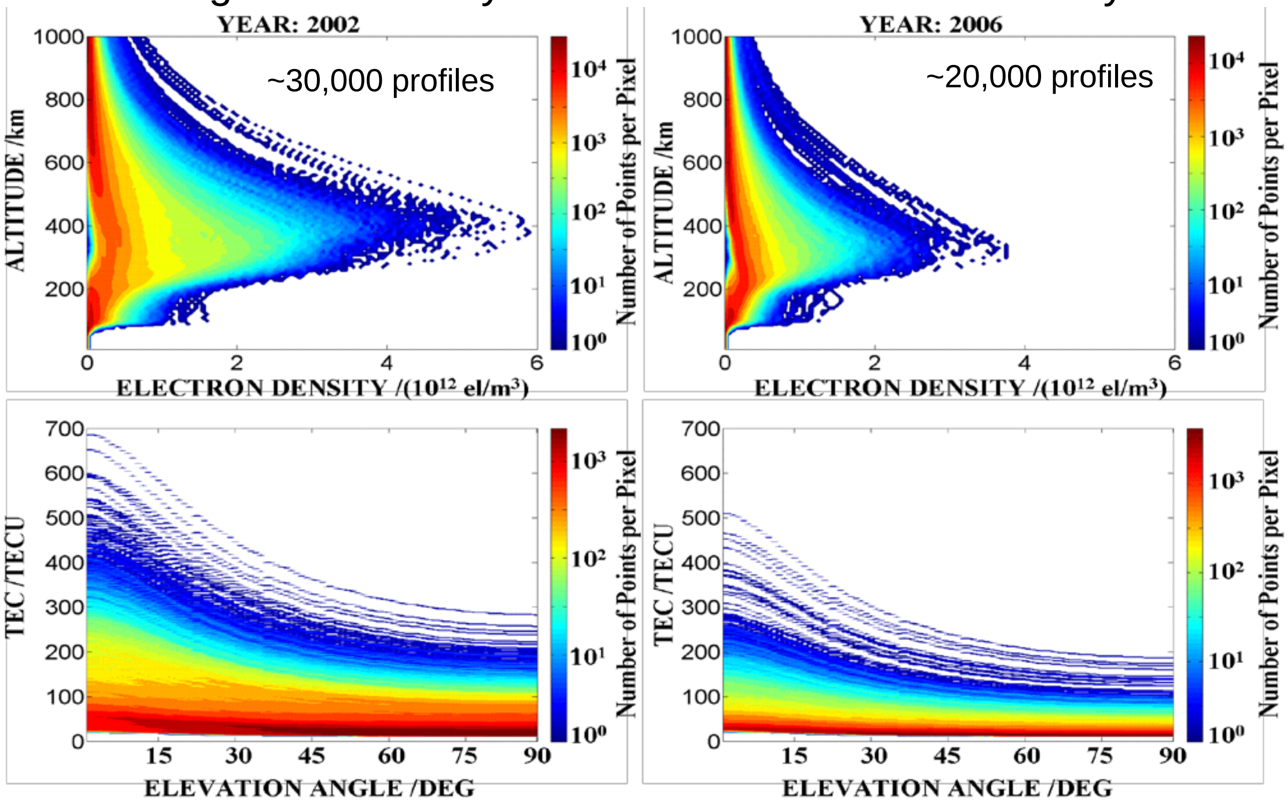

Data provided via http:/swaciweb.dlr.de/

Intercomparison between maximum electron density NmF2 retrieved from different satellites

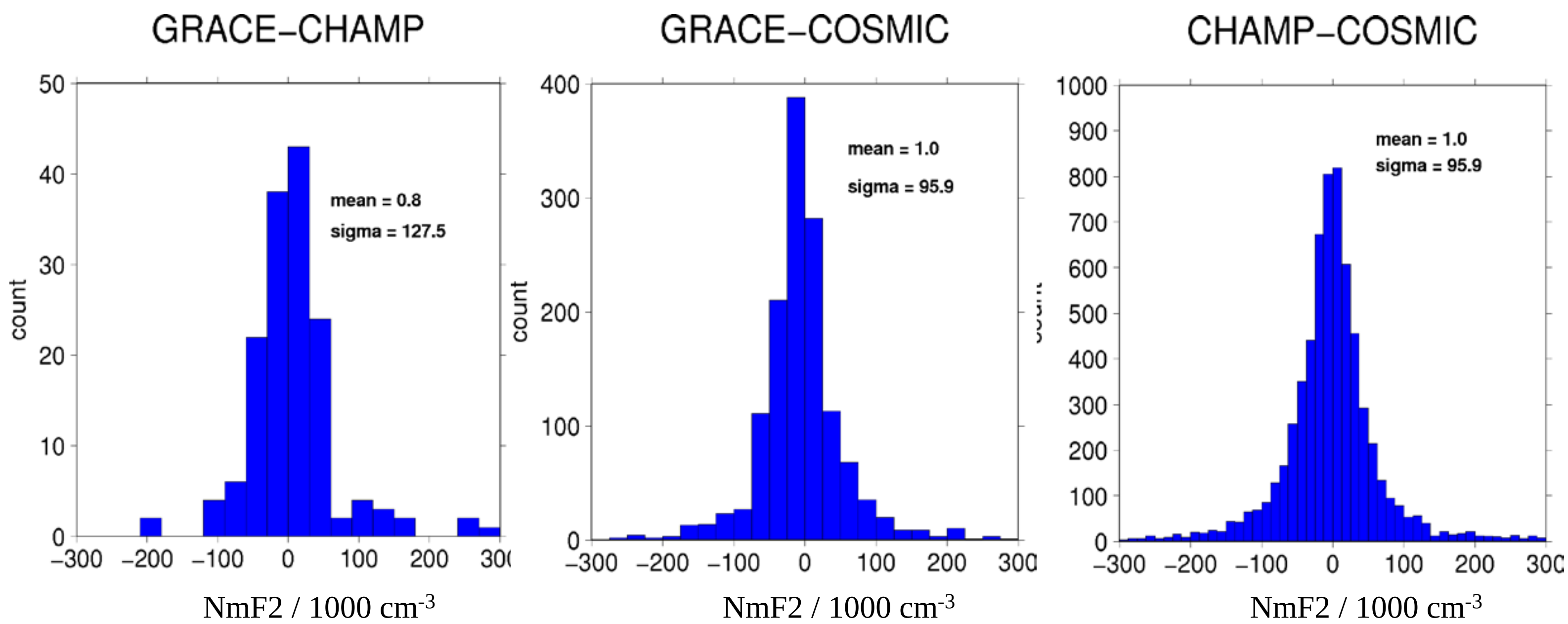

- Good agreement of NmF2 retrievals from different satellites
  - Bias < 1 $x10^3$ cm^{-3}
  - Standard deviation < 1.3 $x10^5$ cm^{-3}
  - GNSS radio occultation measurements provide consistent data sets

Topside ionosphere / plasmasphere sounding

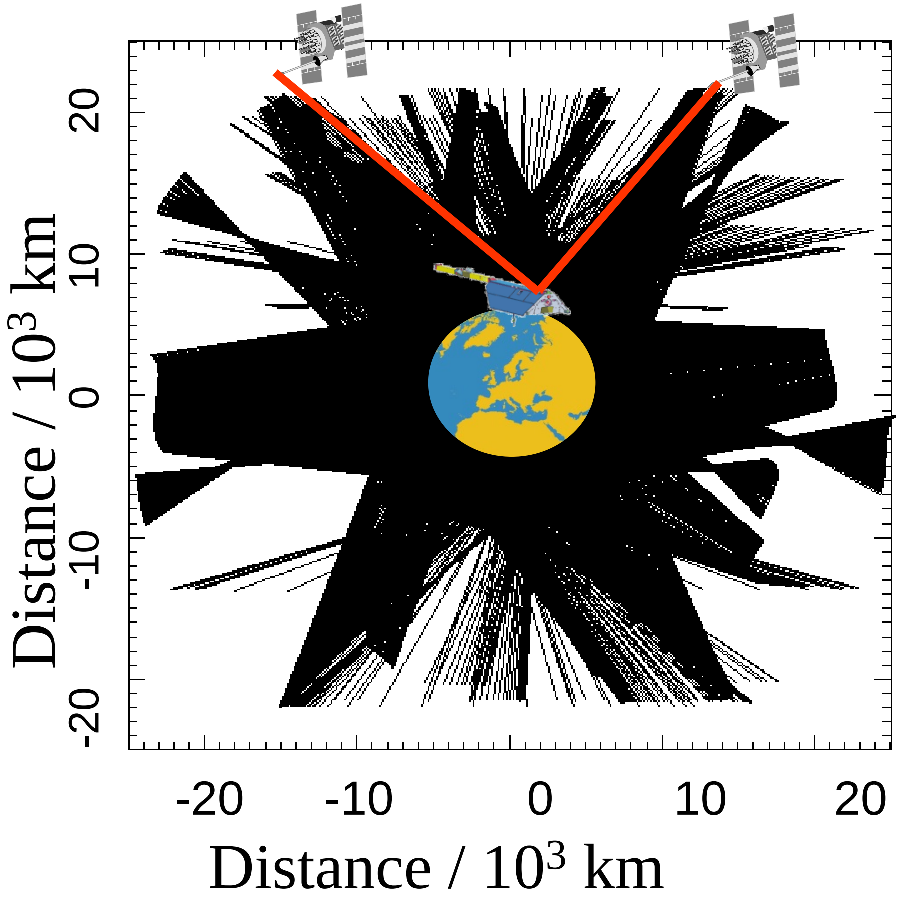

2D projection of a typical radio link distribution for a full CHAMP revolution within 93 minutes.

The GPS navigation data measured onboard CHAMP (0.1 Hz sampled) provide up to about 3000 measurements during one revolution.

Assimilation of the TEC data obtained for one revolution into the PIM model reveals the 2 D electron density distribution close to the CHAMP orbit height.

[REF 09]

Reconstruction of the electron density distribution

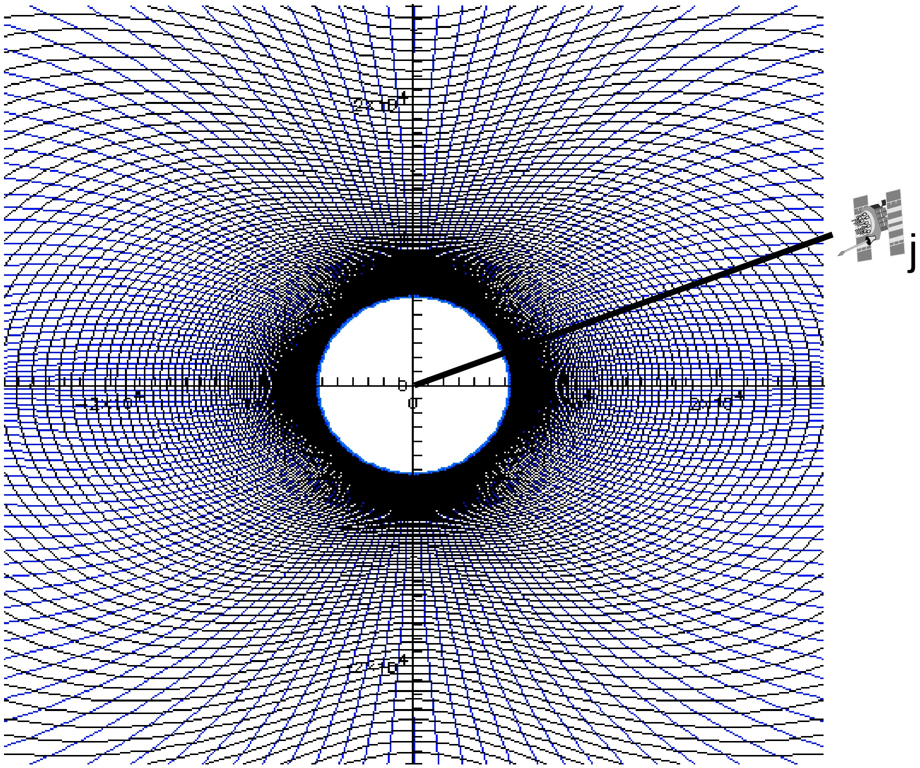

Voxel structure for data assimilation

Discretization for ray path j:

$$TEC_j = \sum_i n_{eij} ds_{ij}$$

TEC = D*X

& Data

PIM assimilation

Electron density distribution

[REF 09]

Electron density distribution in CHAMP orbit plane

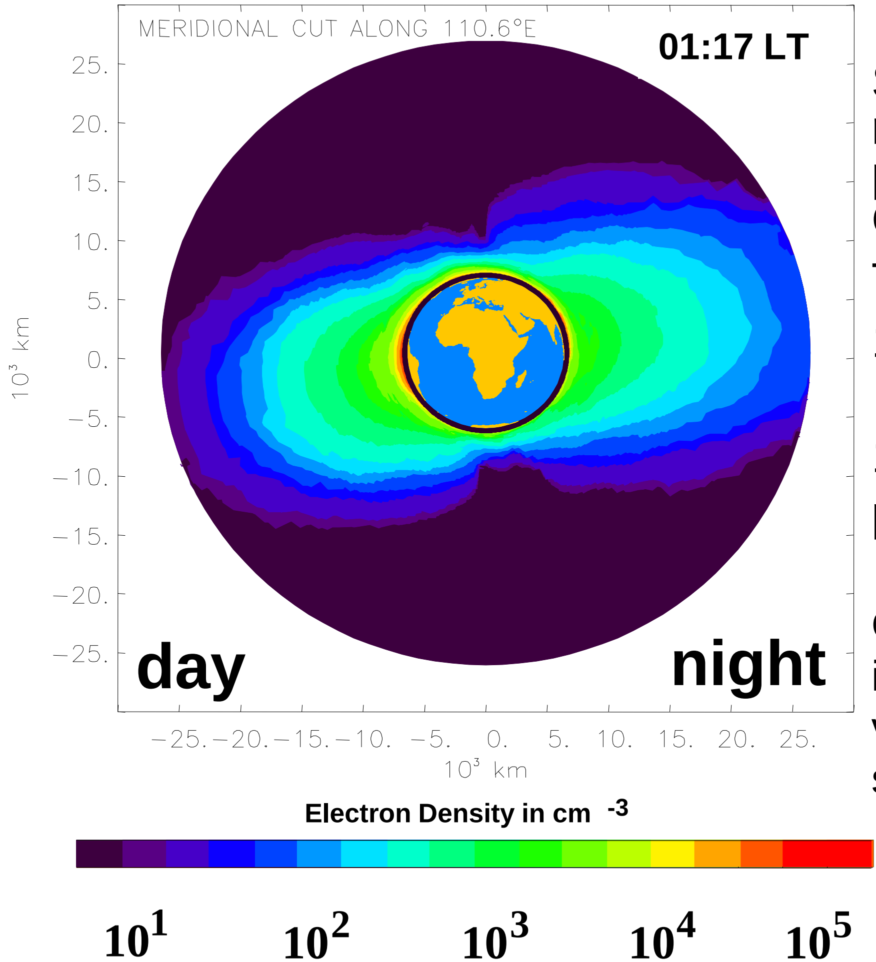

Shown is an average reconstruction of the Geo-plasma distribution from CHAMP to GPS orbit heights

Time interval:

14 -23 August 2005

15-16 3D images are generated per day

Operational images imaging provided via SWACI since June 2005

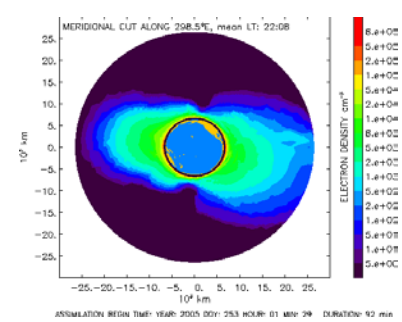

Outline

- Introduction
- Radio wave propagation and ionosphere
  - The ionosphere
  - Fundamentals of radio wave propagation
- Probing the ionosphere and space weather relationships
  - Ground based
  - Radio occultation
  - Topside ionosphere/plasmasphere monitoring
  - Observations
- Ionospheric impact on radio systems and mitigation techniques
  - Telecommunication
  - Remote sensing
  - Space based navigation
- Summary

Data base for ionospheric research and modeling

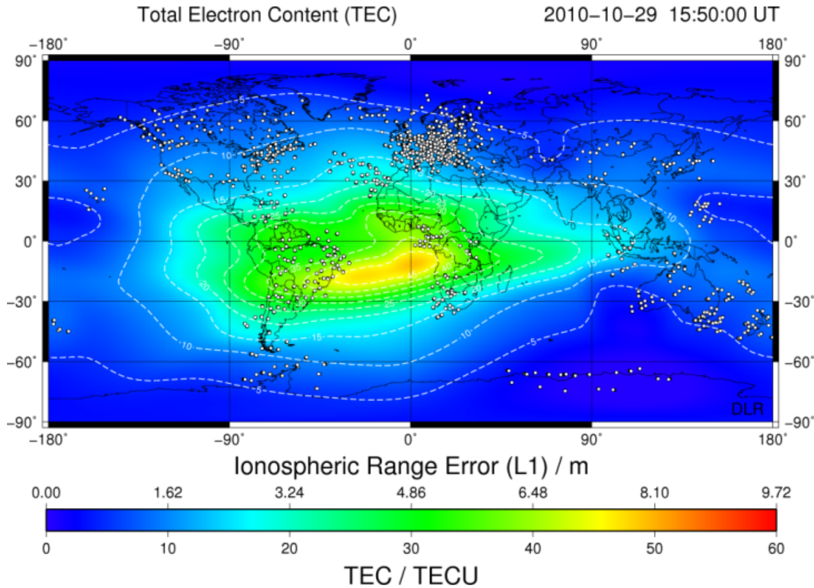

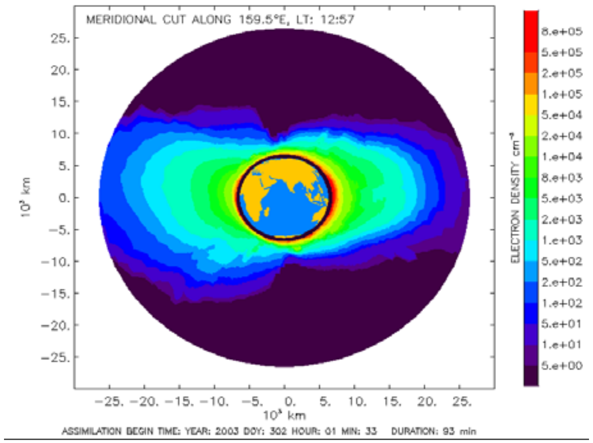

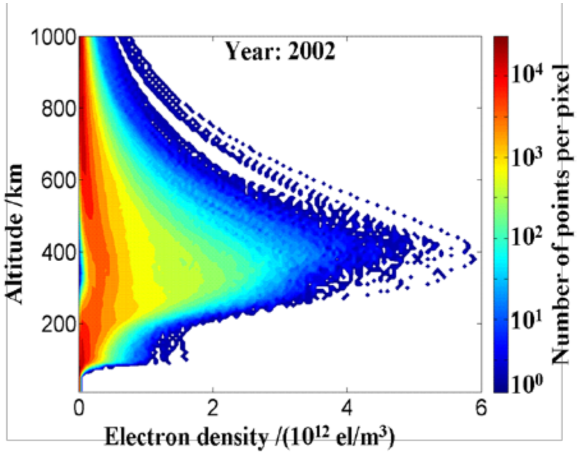

Data base obtained from ground and space based GNSS measurements in the Space Weather Application Center - Ionosphere (SWACI) of DLR

[REF 10]

DLR

TEC dependence from solar activity

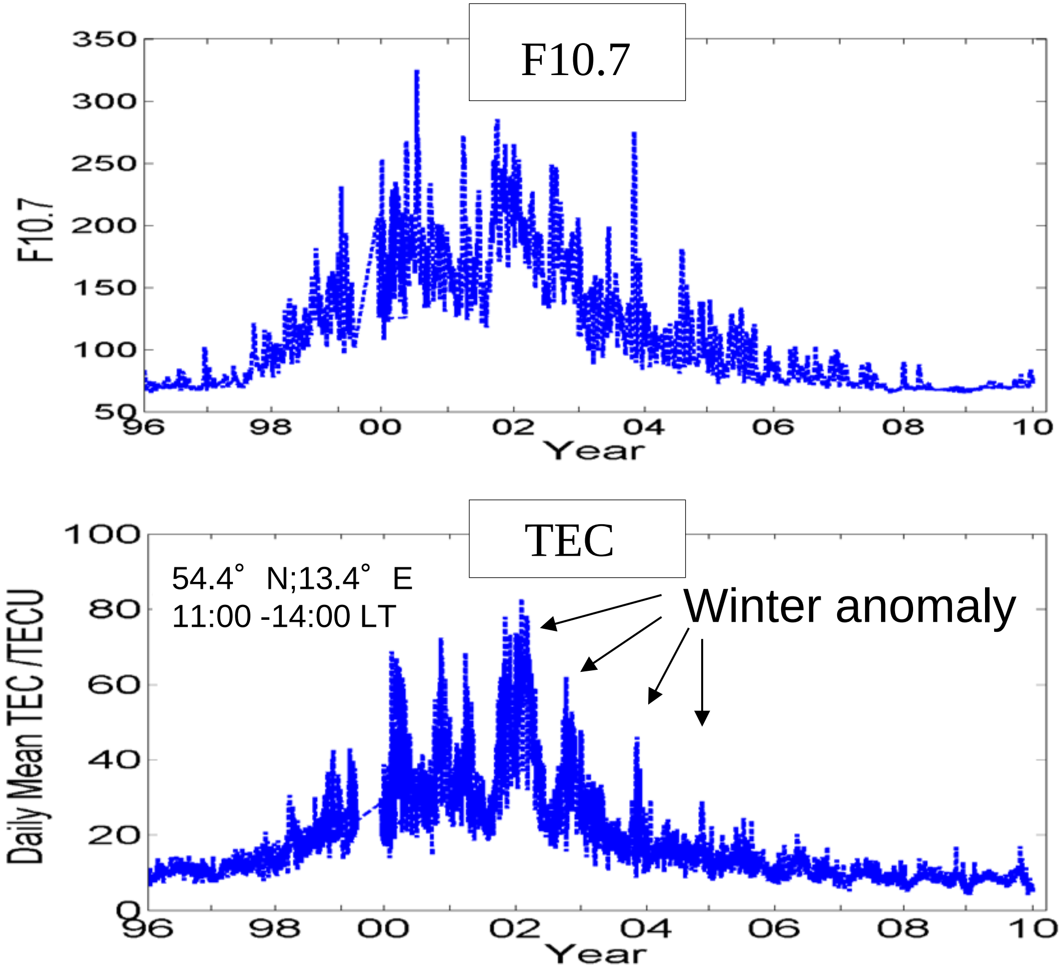

Observed is a strong correlation of TEC with the Solar radio flux F10.7

Solar radio emission is strongly correlated with ionizing EUV flux

F10.7 is input parameter for models to characterize the solar activity

Solar eclipse in TEC on 11 August 1999

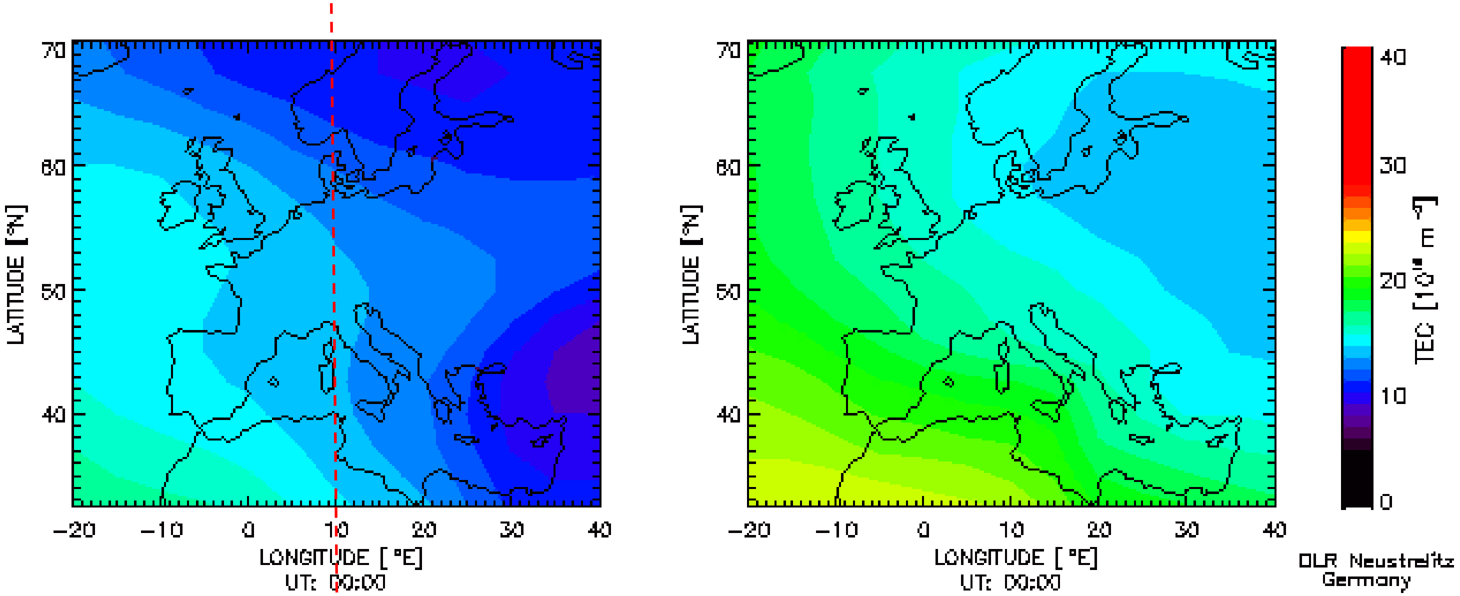

TEC at 11 August 1999

TEC Medians of August 1999

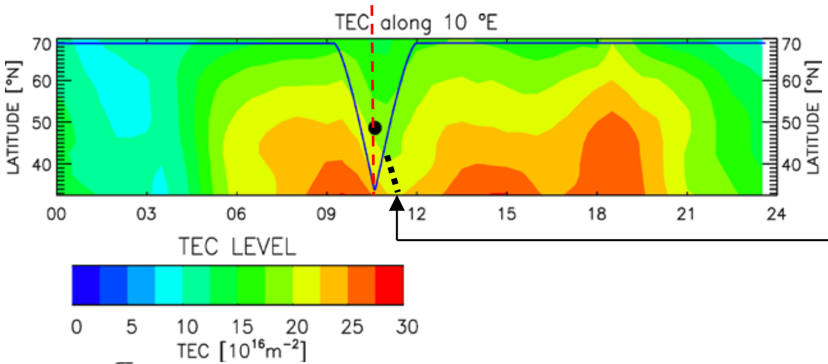

- Solar eclipse can be considered as an activve experiment for studying ionospheric processes
- The ionospheric response is delayed up to 30 minutes

[REF 11]

Solar flare precursor of storm on 28 October 2003

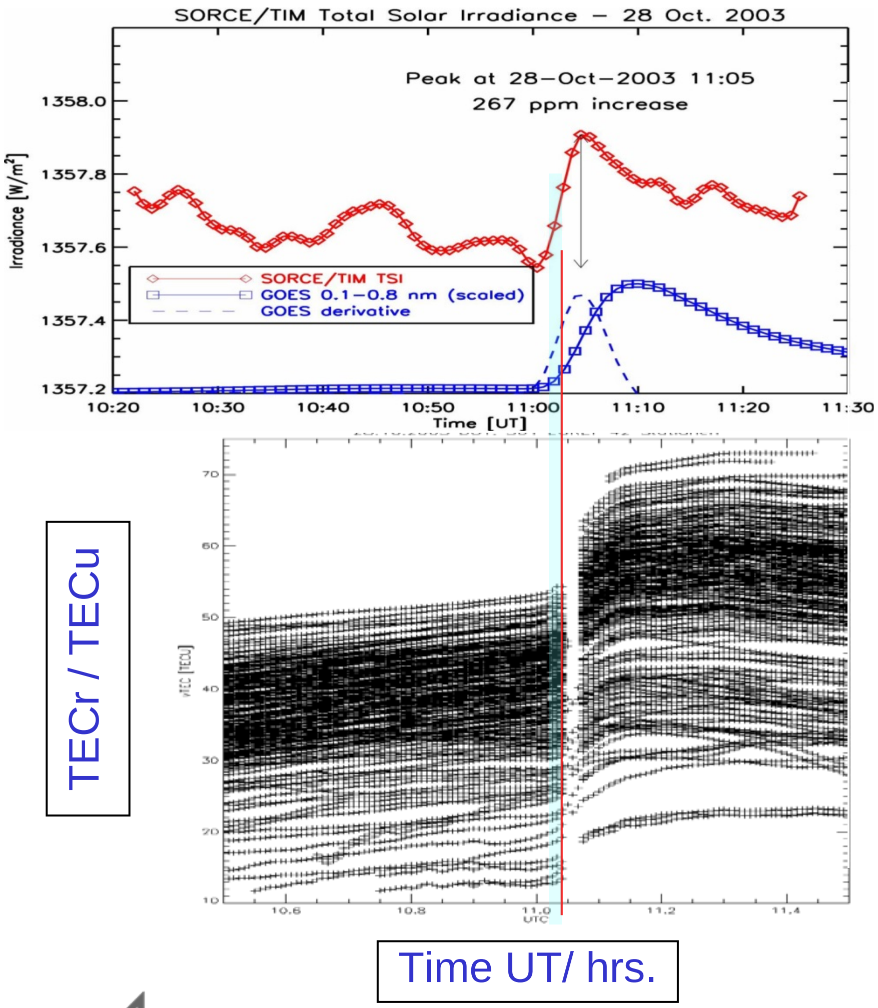

- Strong Solar Flare was observed on 28 October 2003 at 11:05 UT
- Total solar irradiation enhances within a few minutes by 267 ppm
- Rapid and strong increase of TEC at all GPS measurements (range error $\leq$ 3.5 m)
- Number of usable GPS stations dropped down from 30 to 7

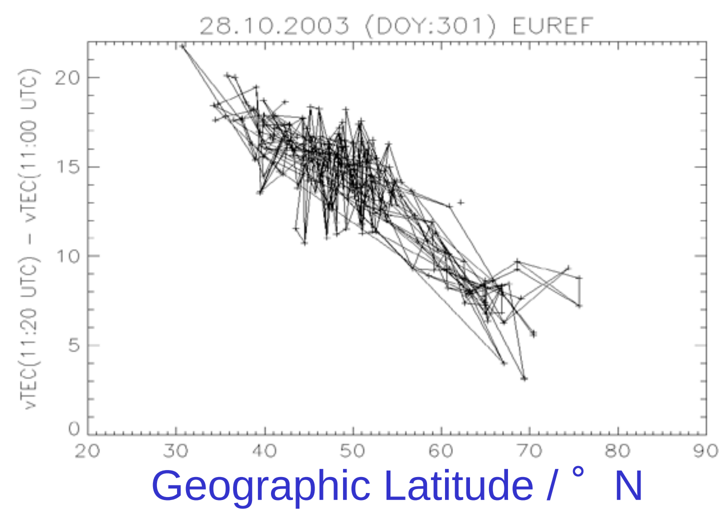

Ionospheric perturbations impacting GNSS

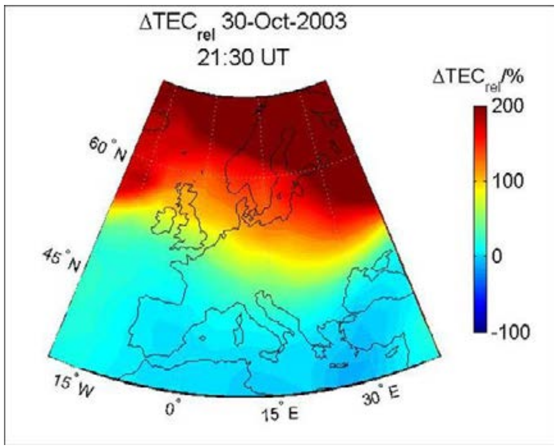

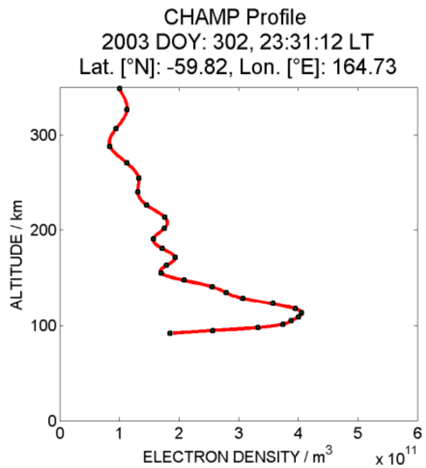

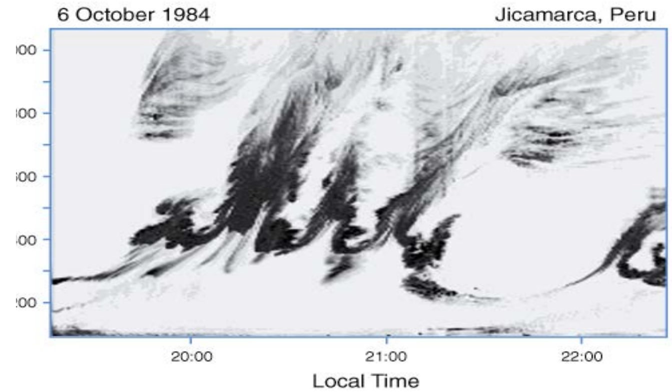

Large scale

- ≈1000 km
- hours
- Propagating Ionisation front
- Horizontal gradients up to 2TECU/km

Mid-scale

- ≈100 km
- minutes
- Wavelike phenomena
- Ionisation patches
- Plasma bubbles

Small scale

- ≤ 10 km
- seconds
- Plasma turbulences
  - Plasma instabilities
  - Particle precipitation

DLR

Ionospheric storm generation and propagation

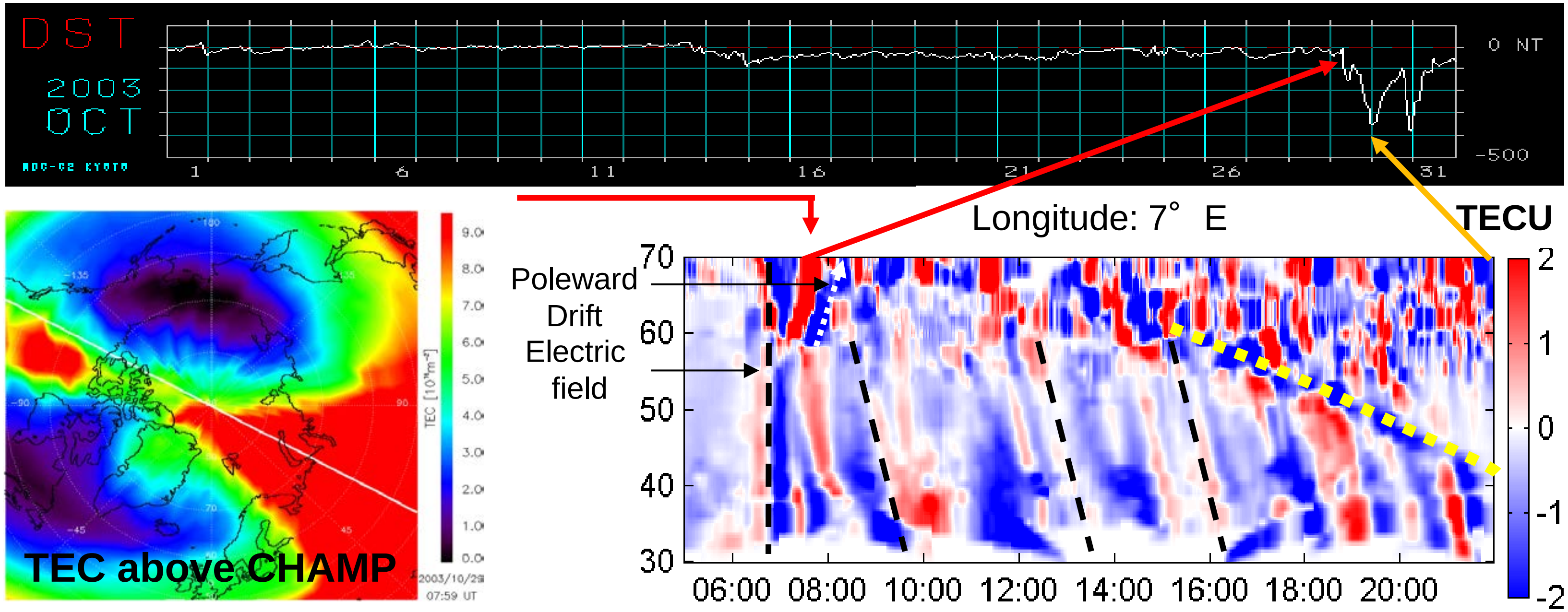

- Immediate response at all latitudes at storm onset
- Tongue of ionization across the Pole
- Wavelike propagation of disturbances during the main phase
- High latitude disturbance zone (northward of the trough) moves equatorward

[REF 12]

Storm on 29 Oct 2003 over Europe and US

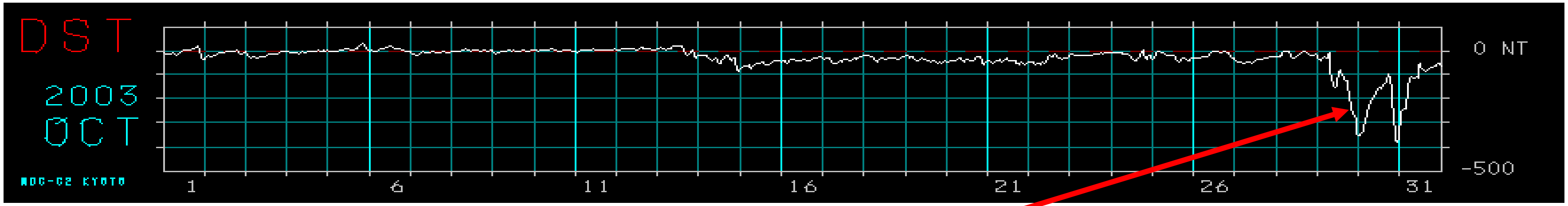

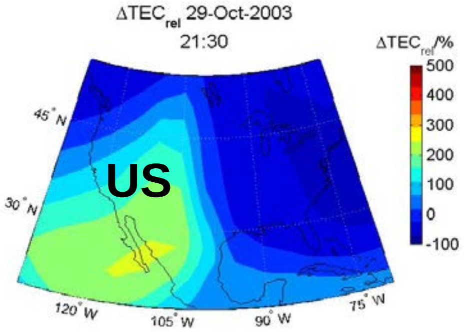

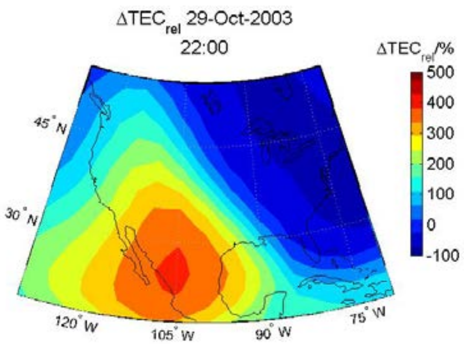

- Different perturbation pattern over Europe and US in the evening hours
- Deviations up to 200 and 500% over Europe and US, respectively

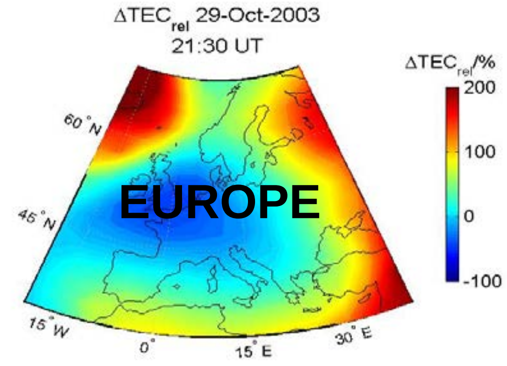

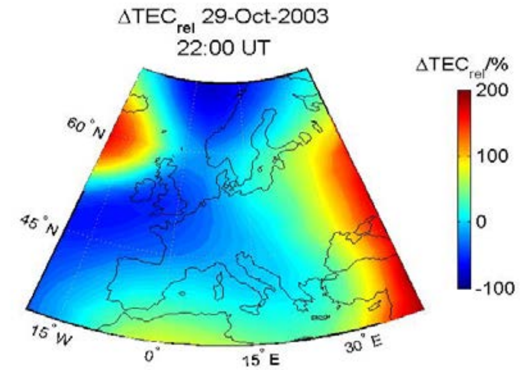

Auroral particle precipitation

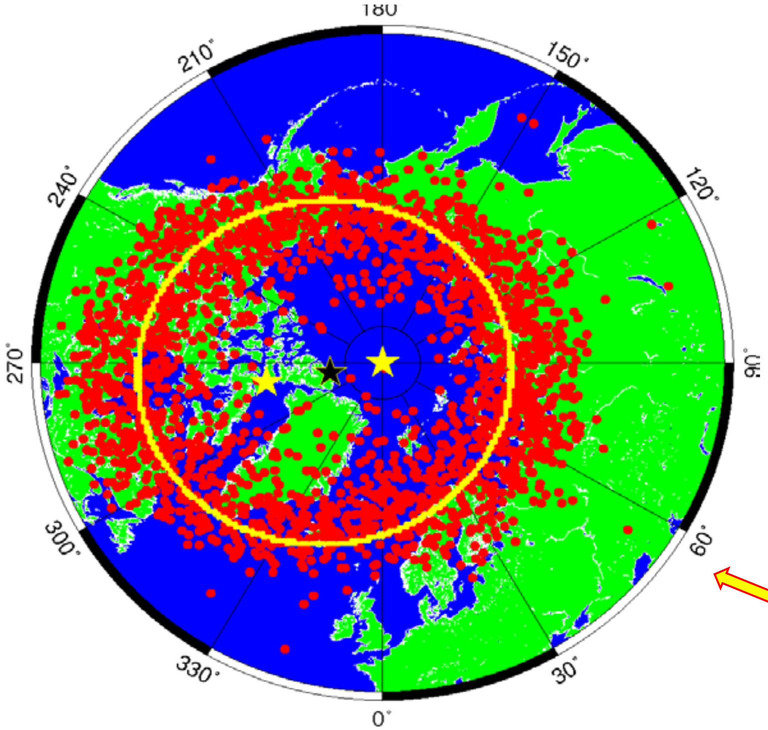

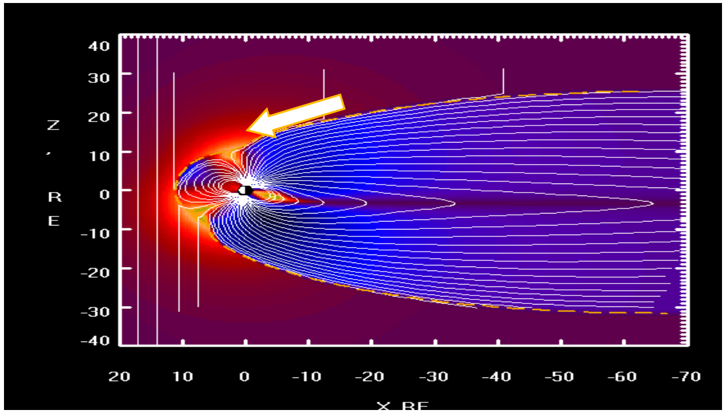

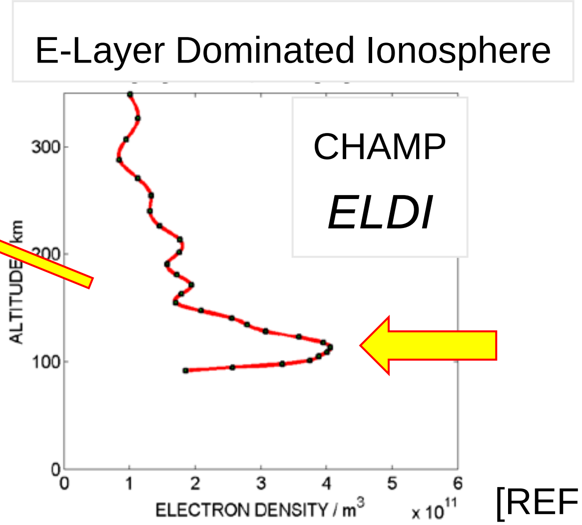

- Particle precipitation from the magnetosphere causes a locally enhanced ionization in the lower ionosphere → gradients, dynamic irregularities

[REF 13]

Small scale irregulariities - radio scintillations

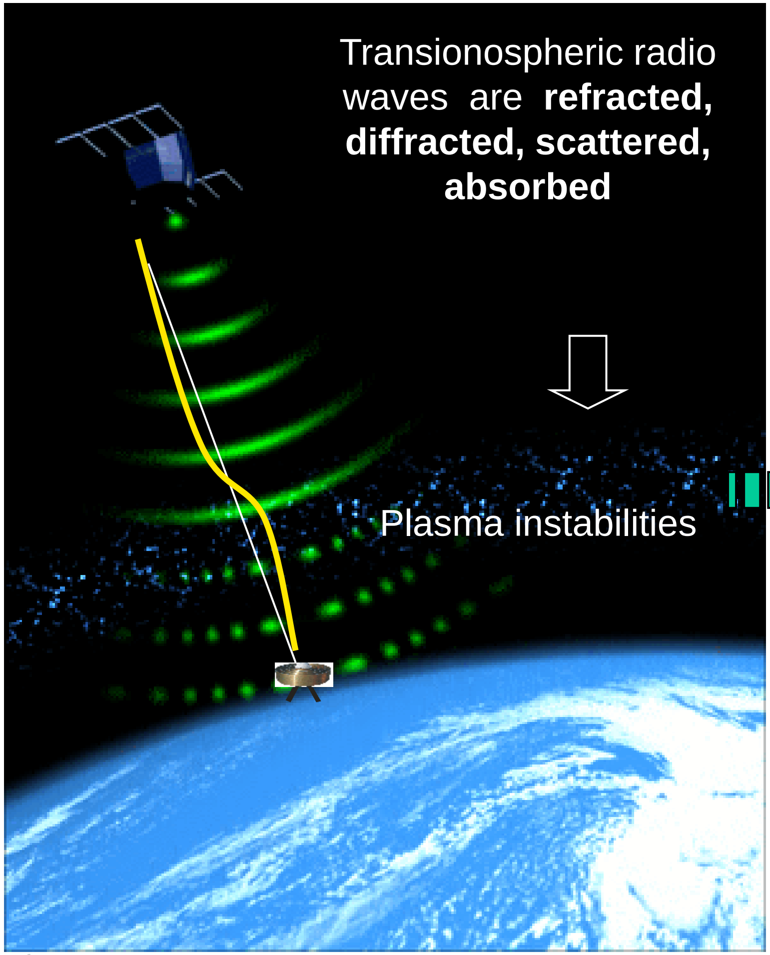

Small scale irregularities and plasma bubbles may cause strong fluctuations of signal strength and phase due to diffracion and forward scattering.

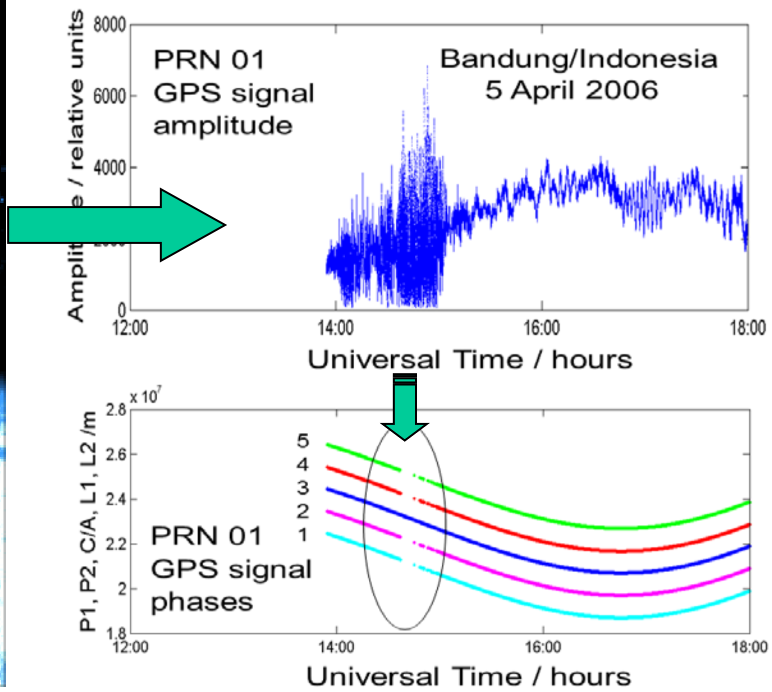

Characteristics of small scale irregularities and related radio scintillations

1st Fresnel zone

$$F_1 = \sqrt{\frac{\lambda \cdot d_1 \cdot d_2}{d_1 + d_2}}$$

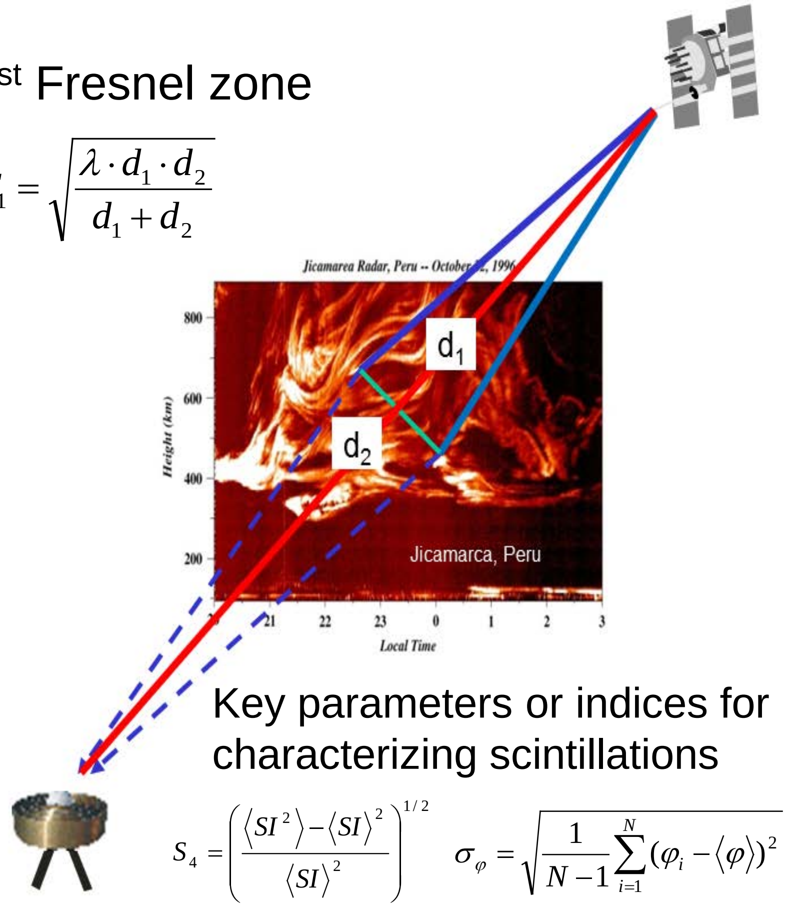

Key parameters or indices for characterizing scintillations

$$S_4 = \left(\frac{\langle SI^2 \rangle - \langle SI \rangle^2}{\langle SI \rangle^2} \right)^{1/2} \qquad \sigma_\varphi = \sqrt{\frac{1}{N-1} \sum_{i=1}^{N} (\varphi_i - \langle \varphi \rangle)^2}$$

- Scintillations occur in all frequency bands
- S_4 amplitudes decrease with increasing frequency ($1/f^{1.5}$)
- At low latitudes scintillations are mainly caused by the Rayleigh-Taylor plasma instability (RTI)
- At high latitudes scintillations are closely related to horizontal gradients of ionisation (TEC)
- Are dependent on various geophysical and space weather factors

Scintillation measurements by GNSS

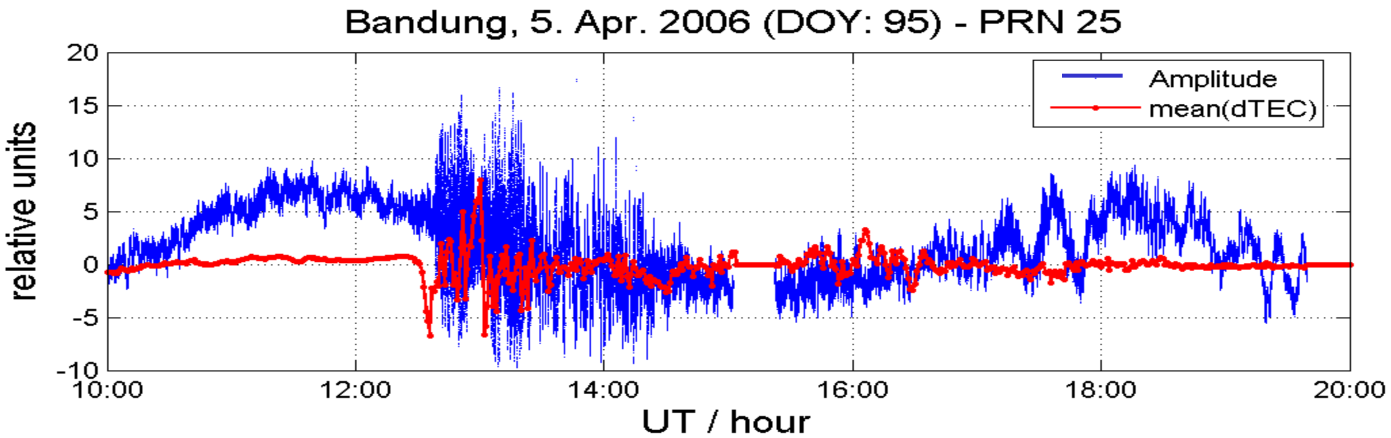

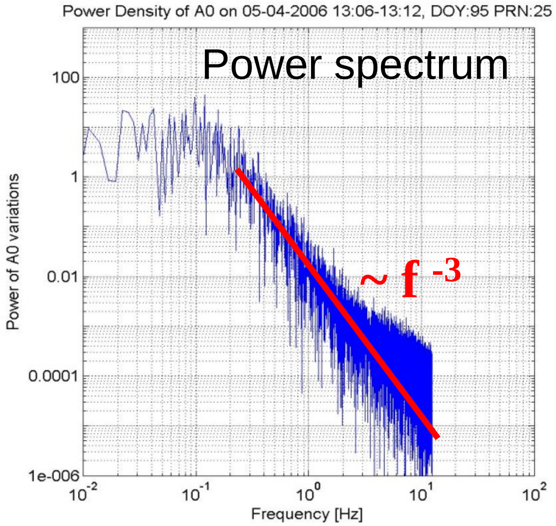

- Szintillations are highly correlated with TEC rate variability at low latitudes.
- Measurements provide information on temporal and spatial characteristics of plasma irregularities and on driving forces of plasma irregularities and bubbles.
- Measurements require receivers with high sampling rate (> 20Hz).
- Coordinated studies with satellite measurements useful (e.g. C/NOFS).

Diurnal variation of scint. activity at low latitudes

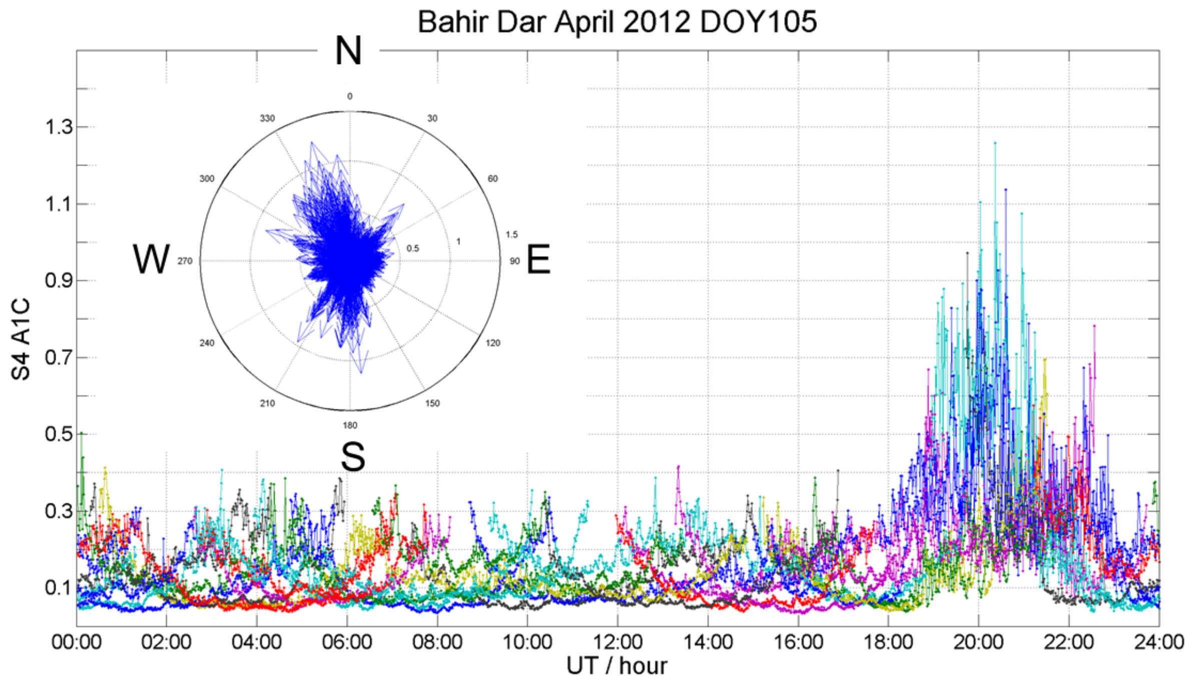

S_4 Scintillation activity enhances regularly in Bahir Dar / Ethiopia at evening hours around 18:00 LT probably due to RTI

Scintillations occur primarily in North-South direction (crest)

Global scintillation activity (S_4)

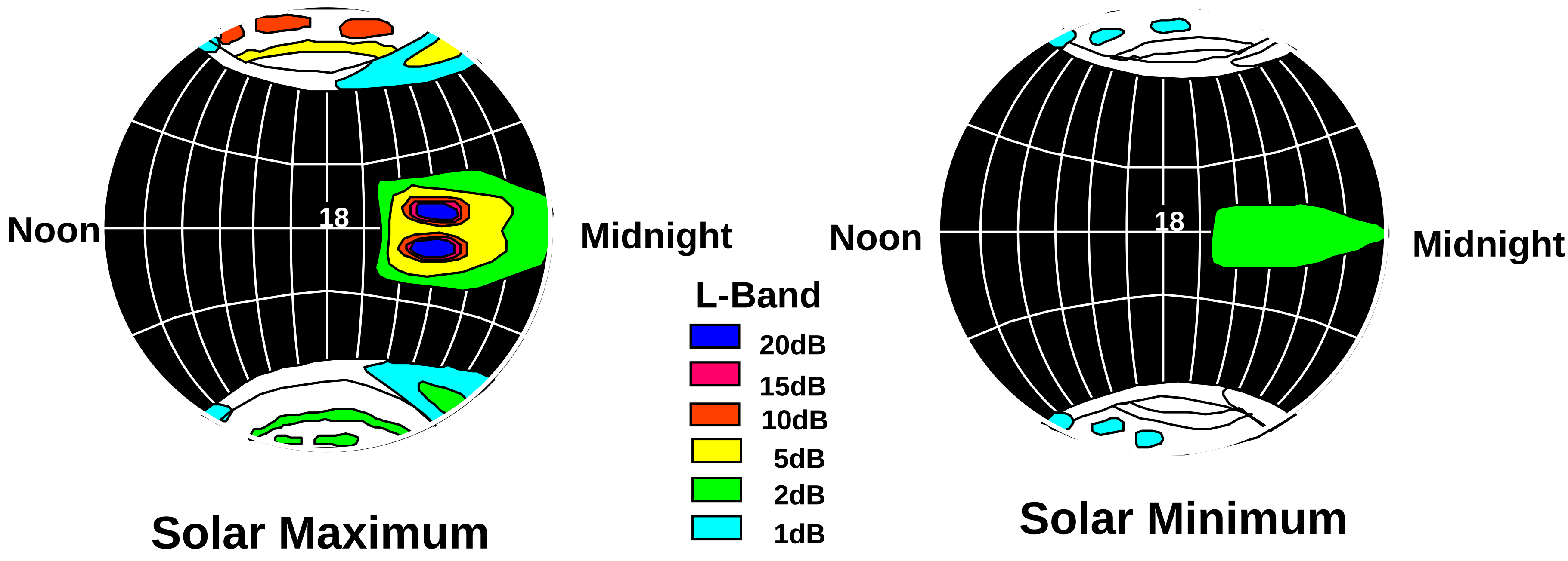

[REF 14]

Outline

- Introduction
- Radio wave propagation and ionosphere
  - The ionosphere
  - Fundamentals of radio wave propagation
- Probing the ionosphere and space weather relationships
  - Ground based
  - Radio occultation
  - Topside ionosphere/plasmasphere monitoring
  - Observations
- Ionospheric impact on radio systems and mitigation techniques
  - Telecommunication
  - Remote sensing
  - Space based navigation
- Summary and conclusions

Review of space weather related ionospheric effects

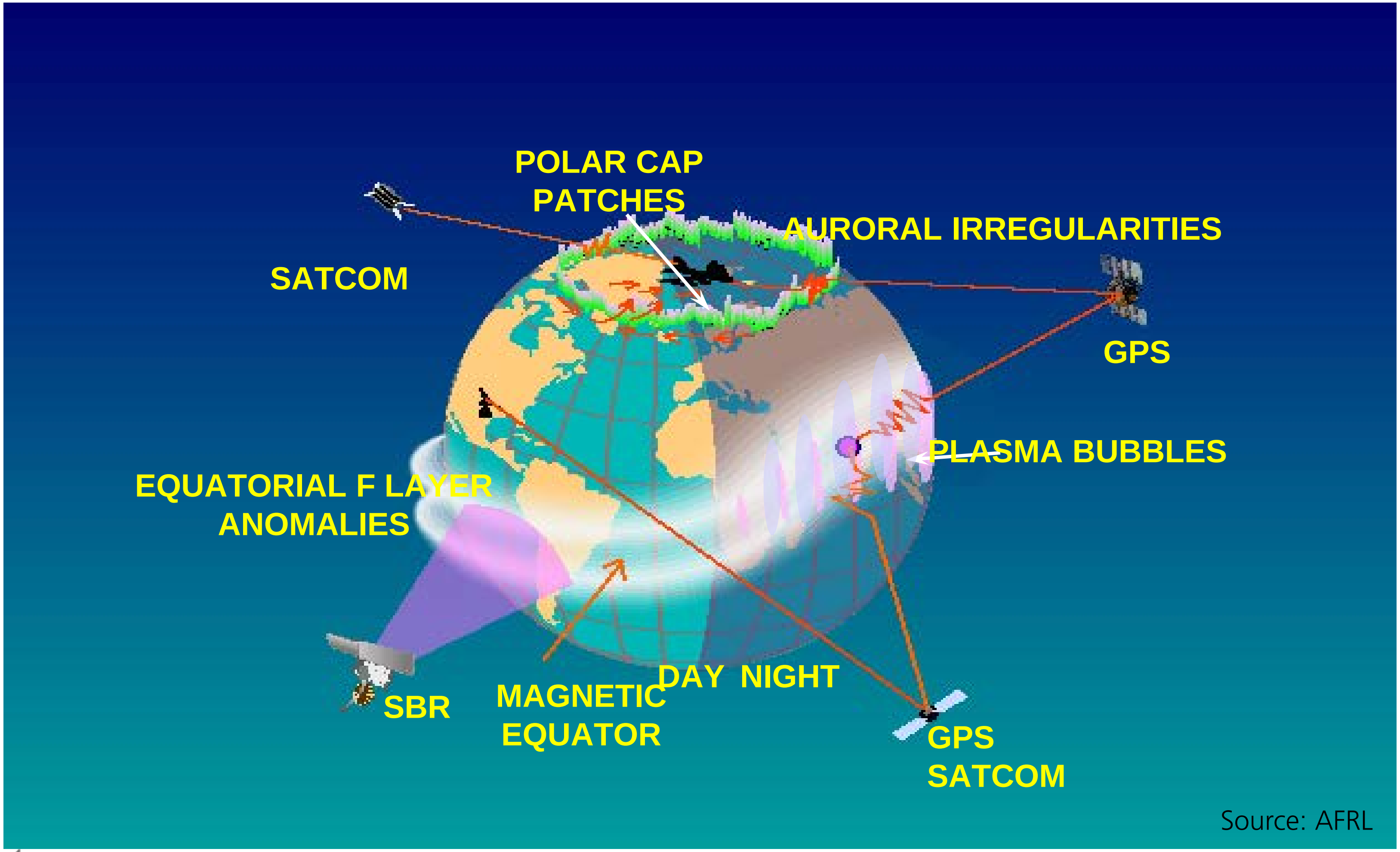

Impact on space based telecommunication

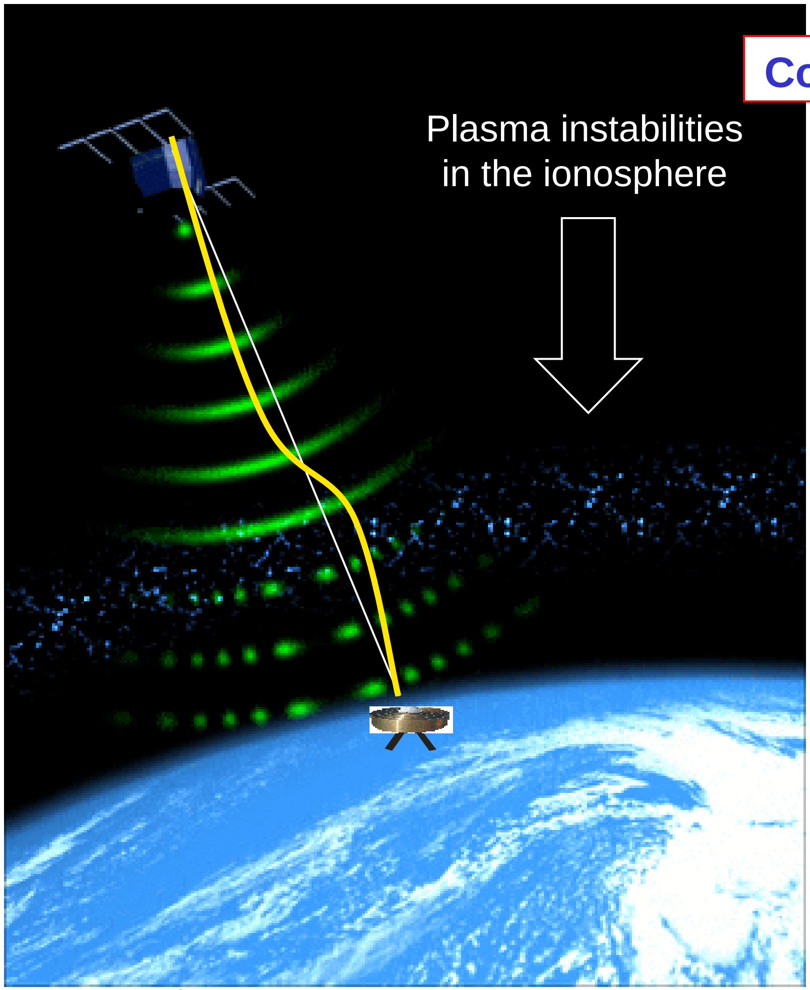

Communication

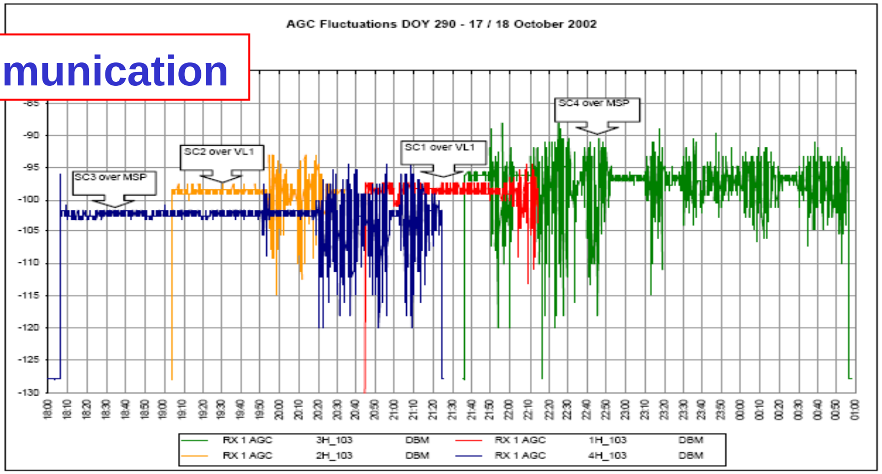

AGC fluctuations affecting all four CLUSTER spacecrafts at different ground stations
(Source: ESOC Report CL-COM-RP-1001-TOS)

Plasma instabilities cause rapid signal strength fluctuations

Loss of lock possible, i.e. interruption of data trasmission and loss of data/information

Impact on terrestrial communication

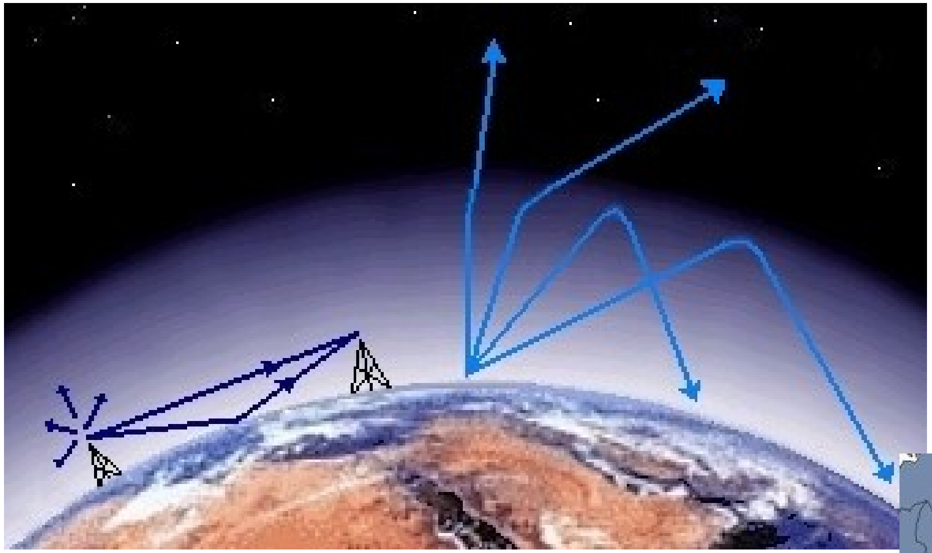

- Radio waves at frequencies below 10 MHz are mostly reflected by the ionosphere
- This results in a long distant propagation of waves
- Solar flares and particle precipitation can prevent the ionosphere from reflecting or refracting radio waves

Short wave radio waves may be absorbed by enhanced plasma density in the lower ionosphere leading to a blackout in radio communications (Short wave fading)

Ionospheric disturbance may enhance long wave radio propagation (measurements of Sudden Ionospheric Disturbances - SIDs)

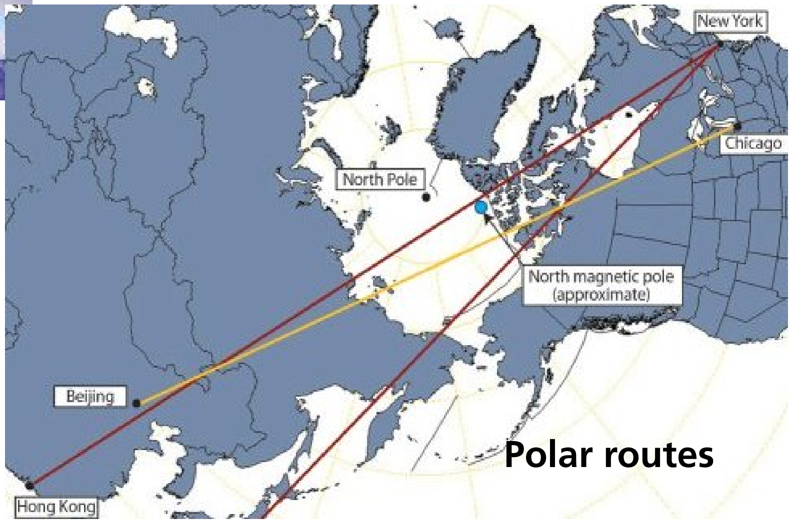

DLR

Student's project:
SOlar Flares by Ionospheric Effects

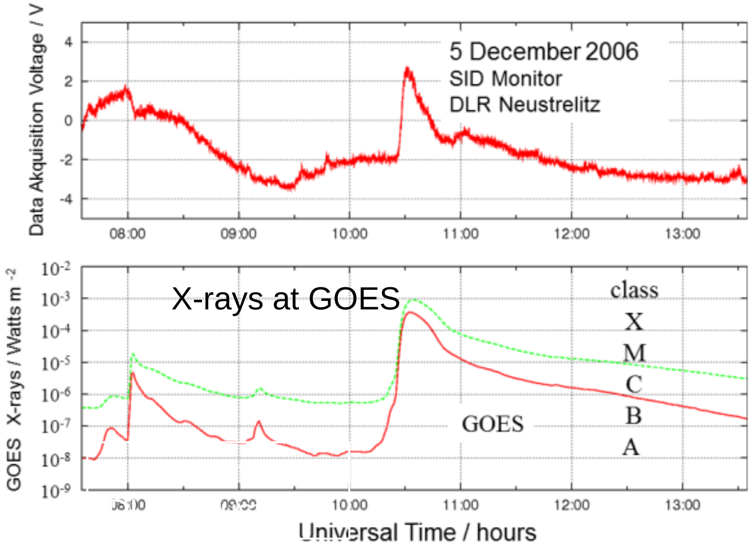

Ionisation of the bottom side ionosphere is modified by X-rays transmitted during solar flares. Related VLF signal strength changes are correlated with X-ray flare intensity measured onboard the GOES satellite.
To monitor flares by VLF measurements within SOFIE, 24 kHz signals of the VLF Station NAA Cutler, Maine, USA are received.

Impact on Remote sensing

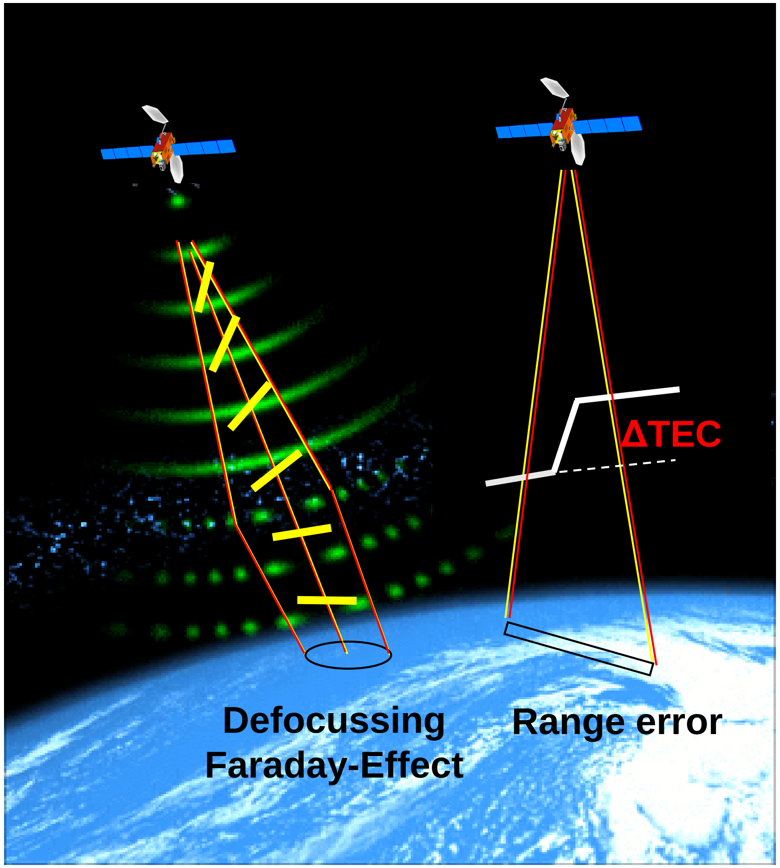

Plasma instabilities cause:

Fluctuations of signal strength
Defocussing of signals.

Anisotropie des Plasmas causes:
Rotation of polarisation plane of linearly polarisied radio signals (Faraday-Effect).

Gradients of TEC cause:
Geometrical distortion of images.

Faraday rotation of radar signals

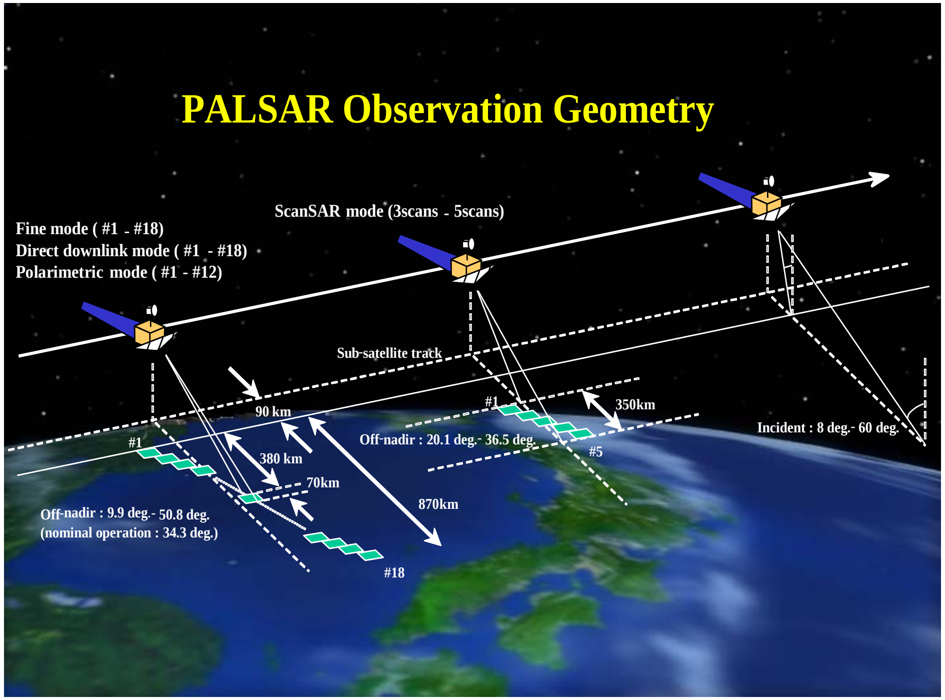

Faraday rotation angle φ_{FR}

$$\varphi_{FR} = \frac{K_F}{f^2} \overline{B \cdot \cos\Theta} \int n_e \, ds$$

Band	f (GHz)	Ω_F [°] (100 TECU)
C	5.0	2
L	1.2	25
P	0.4	200

Development of methods and algorithms for correcting and mitigating of ionospheric propagation errors, e.g. Faraday rotation angle, needed.

DLR

Near real time correction of navigation errors

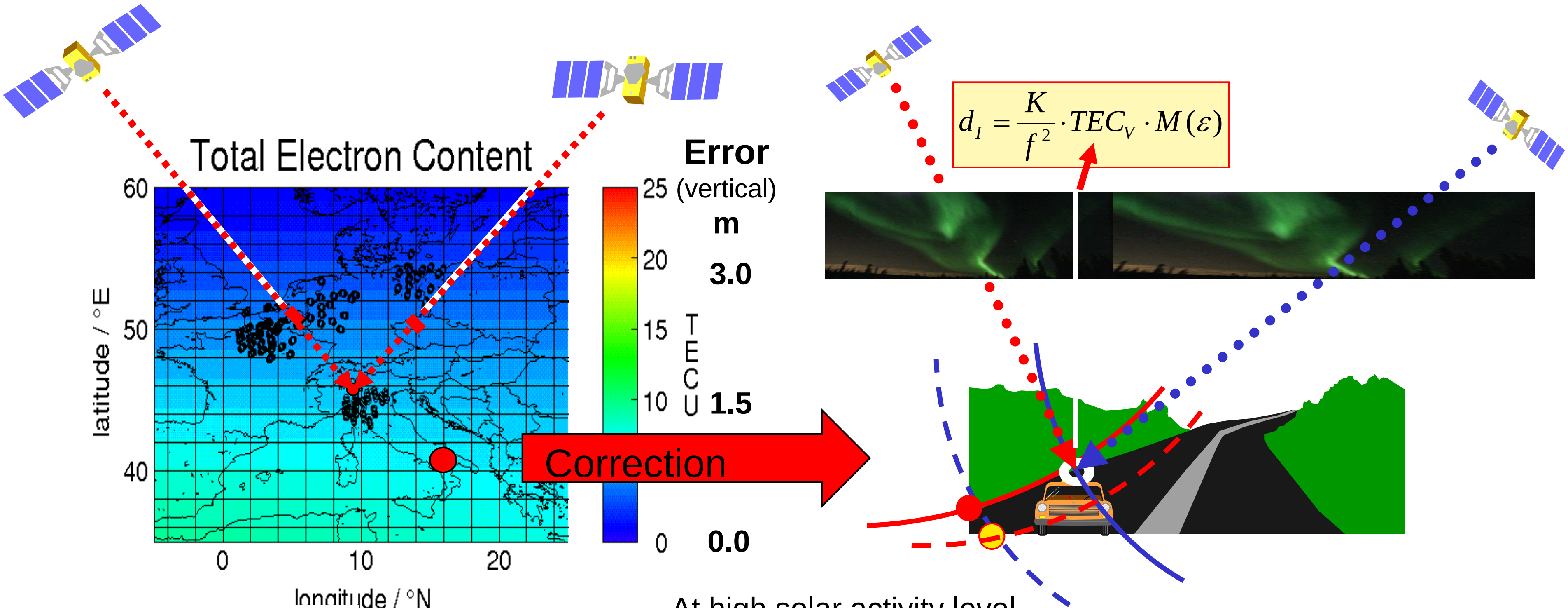

16 GPS stations Time: 01:04:00 UT

At high solar activity level
Vertical errors up to **35 m** possible!

Near real time **TEC monitoring** data can be used for correcting single frequency GNSS measurements.
Data base provided by geodetic networks such as the International GNSS Service (IGS), EUREF and national networks.

Range error correction by ionospheric models

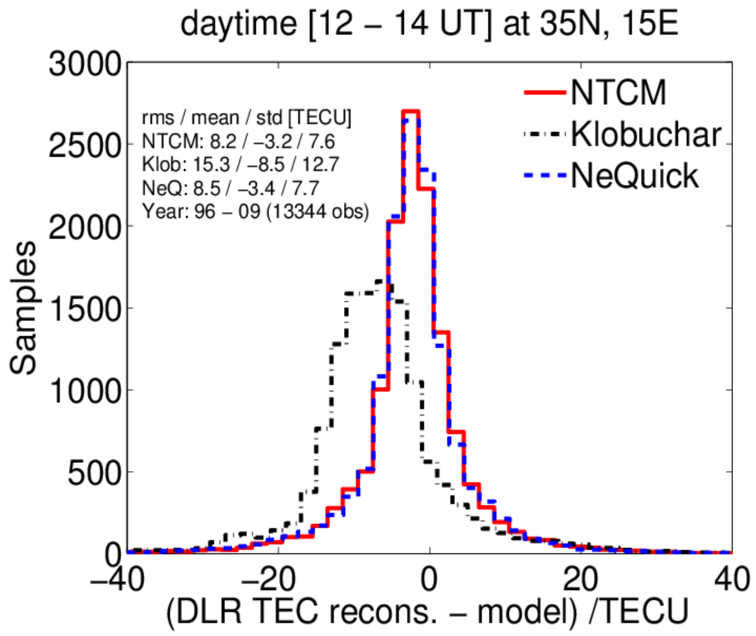

12 coefficient NTCM-GL reaches similar performance as NeQuick (Galileo correction model).

For estimating the ionospheric time delay or range error in Global Navigation Satellite Systems several correction models can be used:

GPS or Klobuchar model
NeQuick model 3D model for Galileo

International Reference Ionosphere (IRI)

Neustrelitz TEC-Models (NTCM- EU, -NP,-SP, -GL

Models provide a climatological correction of propagation errors of about 60%.

[REF 15]

Impact on differential GNSS networks for precise positioning - I

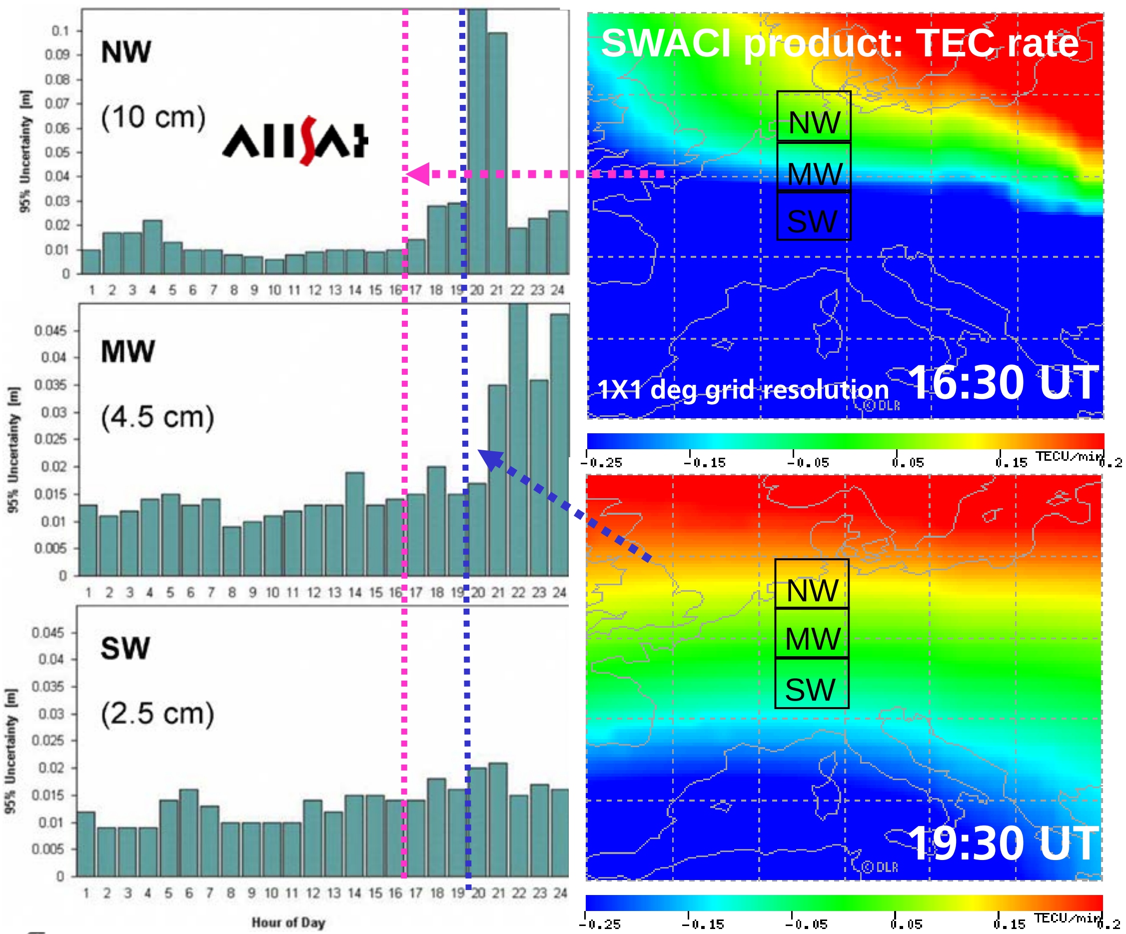

- Performance of the DGPS network of Allsat/Germany (left panel) compared with TEC rate maps from SWACI over Europe on 25 July 2004 at 16:30 and 19:30 UT.

- Accuracy reduces in the same way as the Travelling Ionospheric Disturbance (TID) propagates southward.

- Forecast of TIDs would allow forecasting performance changes.

Impact on differential GNSS networks for precise positioning - II

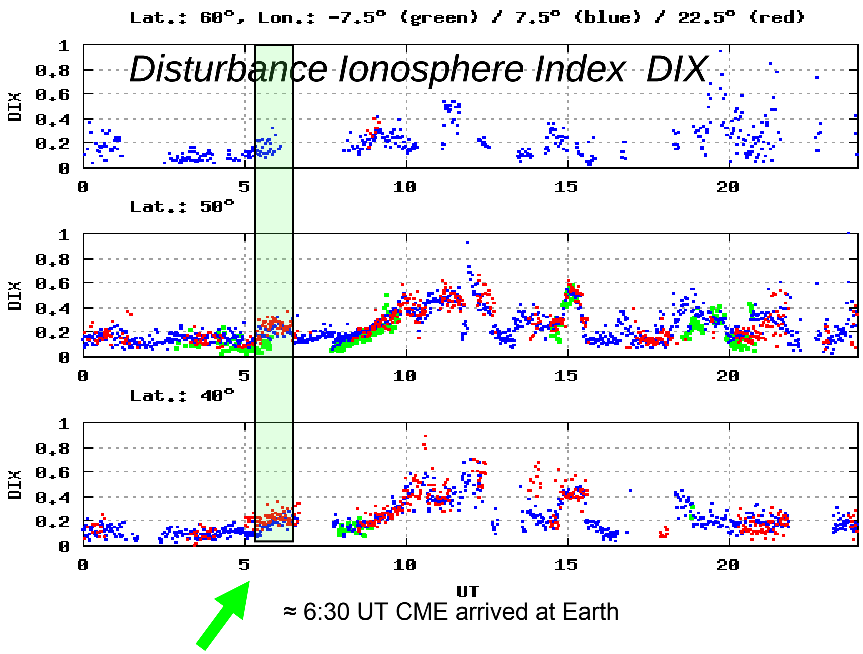

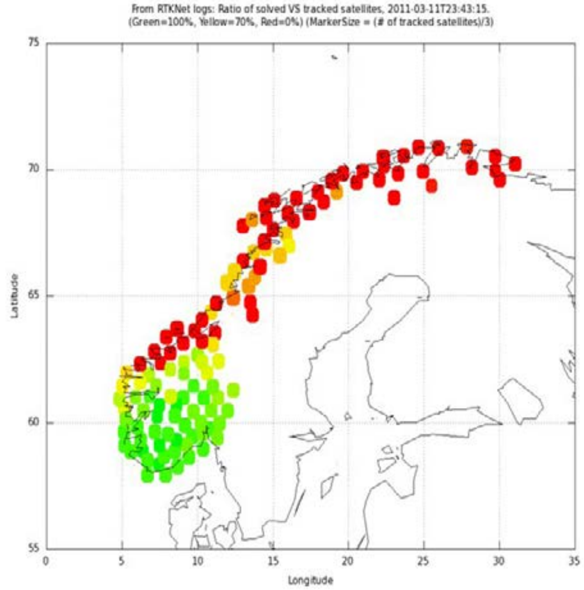

Disturbance Ionosphere Index (DIX) indicates perturbations over Europe which lead to performance degradation at higher latitudes.

Performance degradation of Norwegian geodetic network CPOS (green: corrections for 100% of satellites, red: 0 %,no solution possible.

[REF 16]

Space Based Augmentation Systems (SBAS)

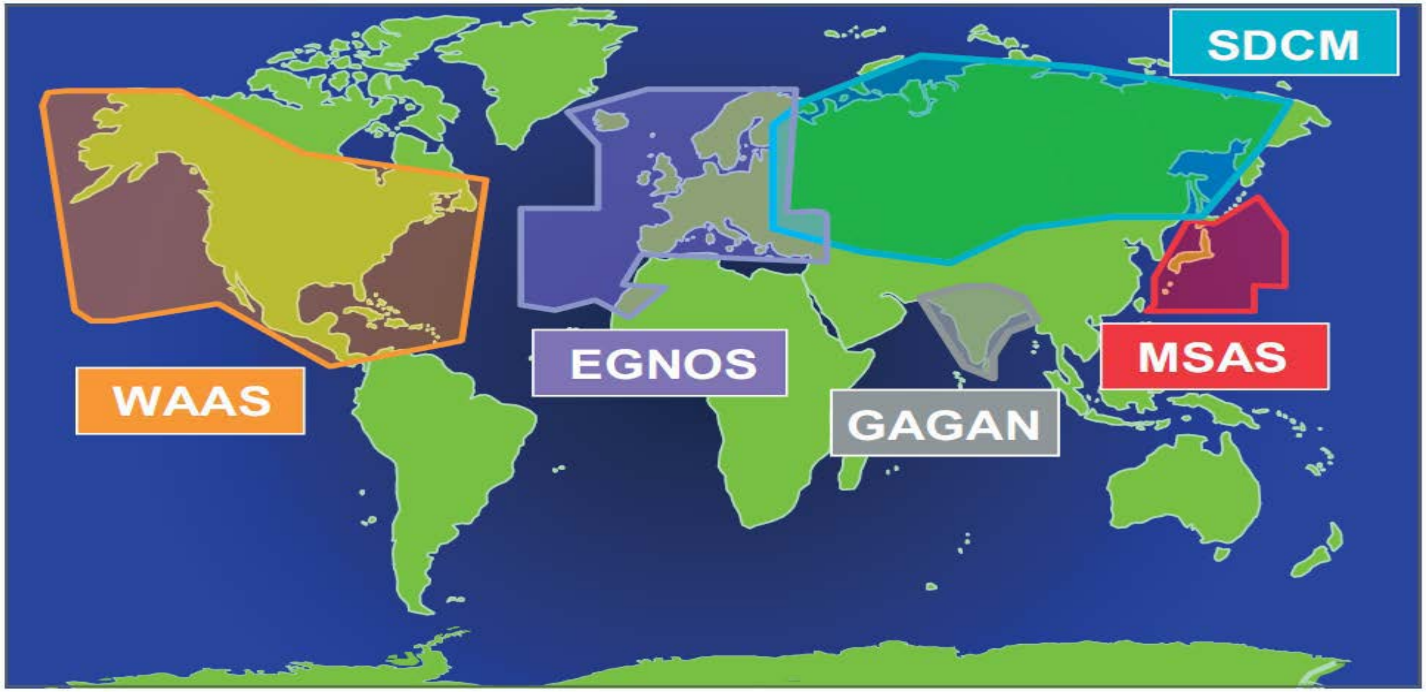

- WAAS (US):Wide Area Augmentation System; since 2003 operational
- EGNOS (Europe): European Geostationary Overlay System; since 2009 operational
- MSAS (Japan): Multi-functional Satellite Augmentation System; since 2007 operational
- GAGAN (India): GPS Aided Geo Augmented Navigation
- SDCM (Russia): System of Differential Correction and Monitoring

Source: ESA

Impact on space based augmentation systems (WAAS on 24 October 2011)

Availability of WAAS 21:00 UT

TEC – TEC median 21:00 UT

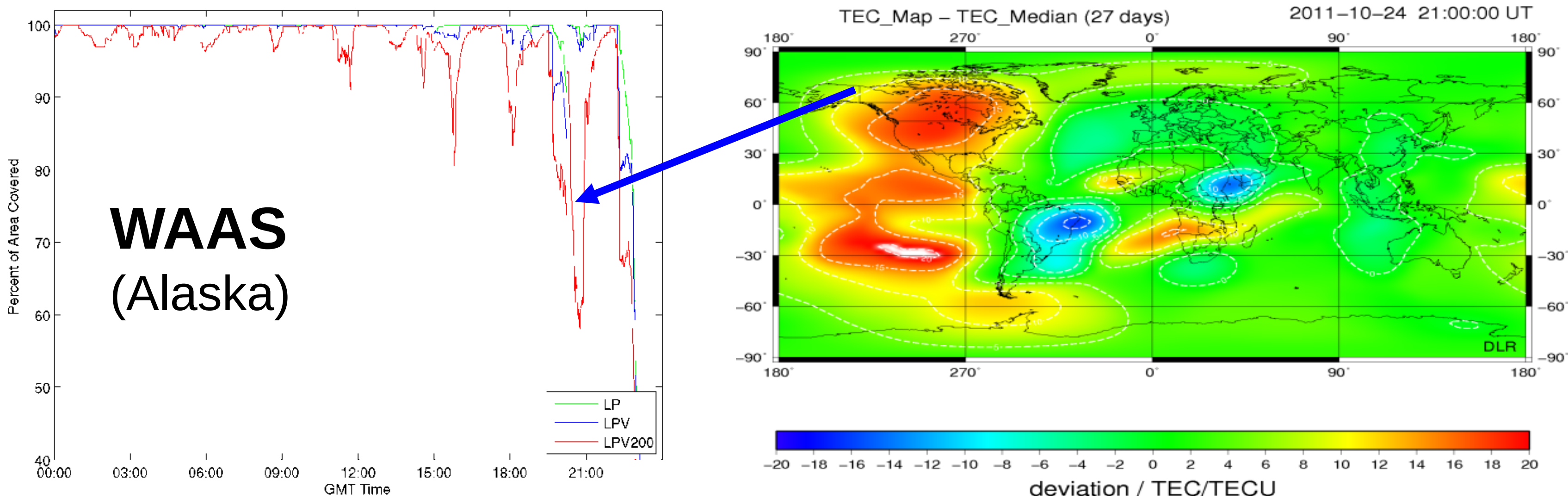

Performance of space based augmentation systems such as WAAS und EGNOS may be strongly affected by ionospheric perturbations

Availability of WAAS /Alaska decreased to less than 60% during the moderate storm on 24 October 2011

Safety of Life (SoL) application - aviation

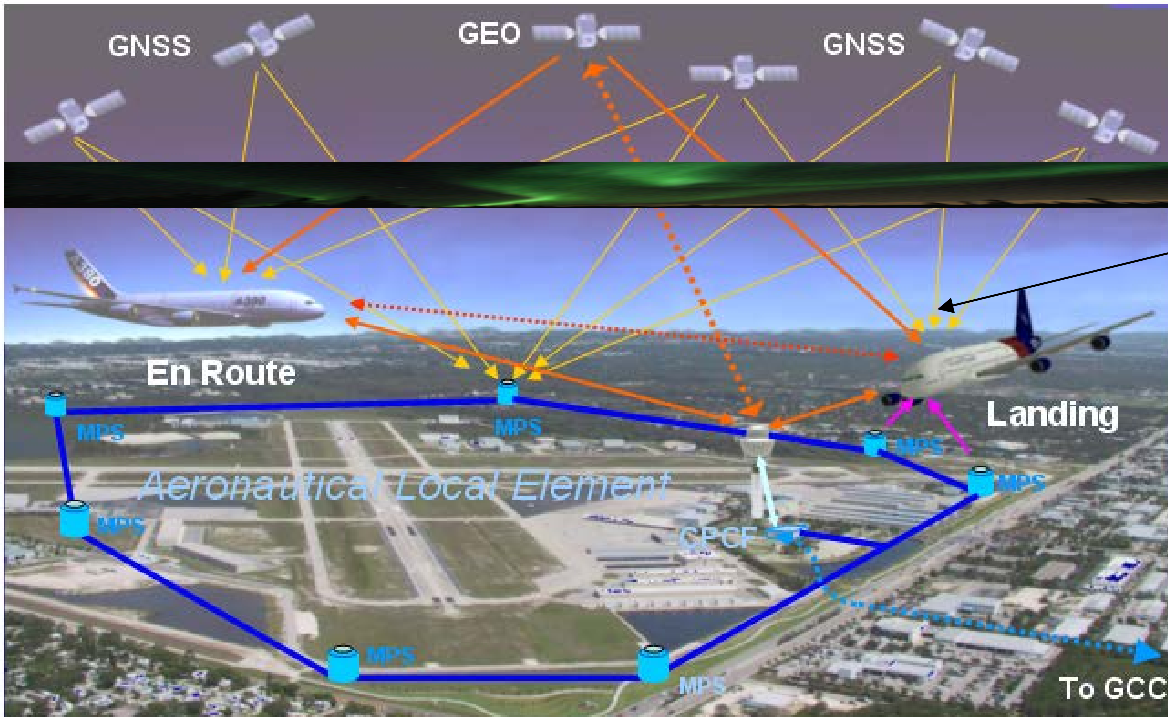

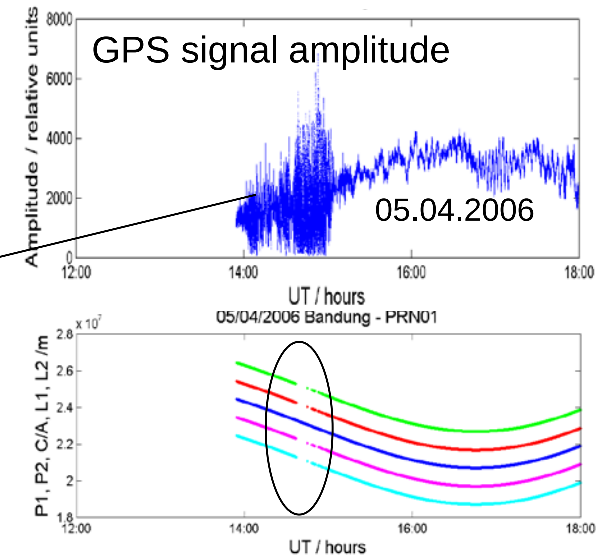

GPS- signal loss

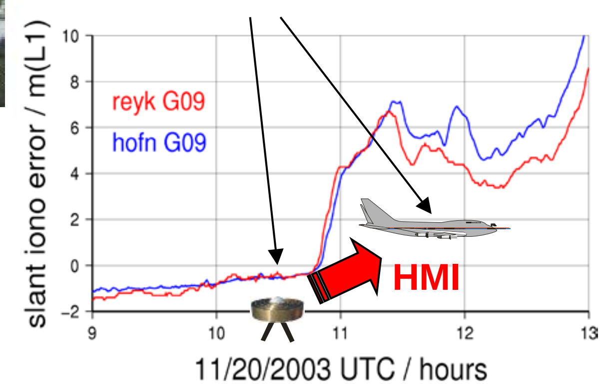

HMI: Hazardous Misleading Information

- Degradation of accuracy, integrity, availability and continuity of signals
- HF Communikation disturbed or interrupted

➡ Operational **detection** and modelling of ionospheric **perturbations** needed

Ionospheric “**Threat-Model**” required

Summary & Conclusions

- Radio signals used in modern communication, navigation and radar systems are impacted by refraction, absorption, diffraction and scattering caused by the ionospheric plasma.
- Ionospheric ionization structure, composition and dynamics, i.e. also radio wave propagation, may seriously be affected by space weather effects.
- Ionospheric delay is the largest error source for single-frequency GNSS.
- Ionospheric storms and related effects such as particle precipitation and TEC gradients may cause problems in precise and SoL applications.
- Modeling, monitoring and forecasting of ionospheric behavior contributes essentially to mitigate ionospheric impact on GNSS.
- Better understanding of ionospheric processes and their coupling is required for further improving mitigation techniques and forecasts.

Thank you for your attention!

Contact:

Dr. Norbert Jakowski
German Aerospace Center
Kalkhorstweg 53
D-17235 Neustrelitz
Germany
Tel. +49 (0)3981 480 - 151
Fax. +49 (0)3981 480 - 123
Email: Norbert.Jakowski@dlr.de
Web: www.dlr.de/kn http://swaciweb.dlr.de

References - I

REF 01 Budden KG (1985) The Propagation of Radio Waves: the theory of radio waves of low power in the I ionosphere and magnetosphere. Cambridge University Press, Cambridge, ISBN 0 521 25461 2

REF 02 Hoque, M.M. and N. Jakowski, Higher Order Effects in Precise GNSS Positioning, Journal of Geodesy, 10.1007/s00190-006-0106-0, 2006

REF 03 Jakowski, N., TEC Monitoring by Using Satellite Positioning Systems, Modern Ionospheric Science, (Eds. H.Kohl, R. Rüster, K. Schlegel), EGS, Katlenburg-Lindau, Berlin, pp 371-390,1996

REF 04 Jakowski, N., C. Mayer, M. M. Hoque, and V. Wilken (2011) TEC Models And Their Use In Ionosphere Monitoring, Radio Sci., 46, RS0D18, doi:10.1029/2010RS004620, 2011

REF 05 Jakowski, N., A. Wehrenpfennig, S. Heise, Ch. Reigber, and H. Lühr (2002) GPS Radio Occultation Measurements of the Ionosphere on CHAMP: Early Results, Geophysical Research Letters, 29, No. 10, 10.1029/2001GL014364

REF 06 Jakowski, N., Ionospheric GPS Radio Occultation measurements on board CHAMP, GPS Solutions (2005) 9: 88–95 DOI 10.1007/s10291-005-0137-7, 2005

REF 07 Hajj GA, Romans LJ (1998) Ionospheric electron density profiles obtained with the global positioning system: results from the GPS/MET experiment, Radio Sci 33:175–190

REF 08 Schreiner, W., C Rocken, S. Sokolovskiy, D. Hunt (2010) Quality assessment of COSMIC/ FORMOSAT-3 GPS radio occultation data derived from single- and double-difference atmospheric excess phase processing GPS Sol. (2010) 14:13–22 DOI 10.1007/s10291-009-0132-5

REF 09 Heise, S., N. Jakowski, A. Wehrenpfennig, Ch. Reigber, H. Lühr, Sounding of the Topside Ionosphere/Plasmasphere Based on GPS Measurements from CHAMP: Initial Results, Geophysical Research Letters, 29, No. 14, 10.1029/2002GL014738, 2002

REF 10 Jakowski, N., S. M. Stankov, D. Klaehn, Operational space weather service for GNSS precise positioning, Annales Geophysicae, 23, 3071-3079, 2005

References - II

REF 11 Jakowski, N., S. Schlüter, S. Heise, J. Feltens, Satellite Technology Glimpses Ionospheric Response to Solar Eclipse, EOS, Transactions. American Geophysical Union, 80, 51, 21 December 1999

REF 12 Jakowski, N., Y. Béniguel, G. De Franceschi, M. Hernandez Pajares, K. S. Jacobsen, I. Stanislawska, L. Tomasik, R. Warnant, and G. Wautelet (2012) Monitoring, tracking and forecasting ionospheric perturbations using GNSS techniques, J. Space Weather Space Clim. 2 (2012) A22, DOI:10.1051/swsc/2012022

REF 13 Mayer, C. and N. Jakowski (2009) Enhanced E-layer ionization in the auroral zones observed by radio occultation measurements onboard CHAMP and Formosat-3/COSMIC, Ann. Geophys., 27, 1207-1212

REF 14 Basu, Su., E. Mac-Kenzie, Sa. Basu (1988) Ionospheric Constraints on VHF/UHF Communication Links during Solar Maximum and Minimum Periods, Radio Sci., 23,3, 363-378

REF 15 Jakowski N, Hoque MM, Mayer C (2011) A new global TEC model for estimating transionospheric radio wave propagation errors, Journal of Geodesy, 10.1007/s00190-011-0455-1

REF 16 Jakowski, N.,V. Wilken, C. Borries, K. S. Jacobsen, and S. Schaefer, Monitoring of the ionospheric storm on 10/11 March 2011 and related impact on the Norwegian positioning network CPOS, ESWW 8 , Namur, Belgium, 2011

REF 12 Hoque, M. M. and N. Jakowski (2011), A new global empirical NmF2 model for operational use in radio systems, Radio Sci., 46, RS6015, doi:10.1029/2011RS004807

REF 13 Hoque M. M. and N. Jakowski (2011), A new global model for the ionospheric F2 peak height for radio wave propagation, Annales Geophysicae 30, 787-809, 2012, doi:10.5194/angeo-30-797-2012

REF 18 Jakowski, N., Mielich, J., Hoque, M. M., Danielides, M. (2010) Equivalent slab thickness at the mid-latitude ionosphere during solar cycle 23, 38th COSPAR Scientific Assembly, 18-25 July 2010, Bremen, Germany